

DYNAMIC RESPONSE OF A SEPARATELY EXCITED DC MOTOR USING  
PARAMETER IDENTIFICATION

by

Swarna Narasimhan

A thesis submitted to the faculty of  
The University of North Carolina at Charlotte  
in partial fulfillment of the requirements  
for the degree of Master of Science in  
Electrical and Computer Engineering

Charlotte

2017

Approved by:

---

Dr. Valentina Cecchi

---

Dr. Yogendra Kakad

---

Dr. Abasifreke Ebong

© 2017  
Swarna Narasimhan  
ALL RIGHTS RESERVED

## ABSTRACT

SWARNA NARASIMHAN. Dynamic response of a separately excited DC motor using parameter identification  
(Under the direction of DR. VALENTINA CECCHI)

DC machines are prone to oscillations or swings in angular speed and armature current due to dynamic changes in the operating conditions, such as excitation and mechanical transients from load or speed variations. In this thesis, a sensitivity analysis-based parameter optimization is applied to a separately excited DC motor to mitigate the swings. A gradient-based criterion minimization method is employed to minimize the gradient of the performance index of the angular velocity and armature current. The optimization is performed on the modeled system and the optimal gain values are fed to the actual system for improved dynamic performance. The angular speed ( $\omega$ ) and armature current ( $I_a$ )-based control approach converges faster reaching optimal gain values compared to the existing  $\omega$  only-based control approach. The effectiveness of the proposed approach is quantified by comparing the integral squared error of the performance index with that of the existing -based control approach. The proposed approach results in a smaller time constant and reduced oscillation damping time, and improves the response of both  $\omega$  and  $I_a$ . The approach promises an efficient swing mitigation in the actual physical system during excitation, speed variations and mechanical transients.

## ACKNOWLEDGMENTS

I would like to thank my advisor Dr. Valentina Cecchi, for her guidance and motivation, without which, this thesis would not have been possible. Her teachings has always been useful and gave encouragement.

It would be my duty to extend my gratitude to the committee members Dr. Yogendra Kakad and Dr. Abasifreke Ebong for taking time to be on my committee and assess my work.

I am also thankful to Dr. Vasilije Lukic for his guidance and EPIC (Energy Production and Infrastructure Center) for its generous support.

## TABLE OF CONTENTS

LIST OF TABLES	vii
LIST OF FIGURES	viii
CHAPTER 1: Thesis Organization	1
1.1 Overview	1
1.2 Objective	2
1.3 Introduction: Chapters	3
CHAPTER 2: Concept of Parameter Optimisation Applied in this Study	5
2.1 Overview	5
2.2 Criterion	5
2.3 Optimality Conditions	7
2.4 Minimization of the criterion with multiple parameters	11
CHAPTER 3: Sensitivity Analysis	13
3.1 Overview	13
3.2 Elementary System Analysis	13
3.3 The Procedure Development	13
3.4 The Analysis of a Multiloop Structure	16
CHAPTER 4: DC Motor Drive Model	21
4.1 Overview	21
4.2 Structure of the DC Motor Drive with Controllers	21
4.3 DC Motor Drive Model Functions	23
CHAPTER 5: Sensitivity Model Applied to a Motor Drive System	26
5.1 Overview	26
5.2 Mathematical Model	27
5.3 Optimization Concept and Block Diagram	29
CHAPTER 6: Optimization Strategy with the Proposed Approach	31

	vi
6.1 Overview	31
6.2 Optimization Strategy	31
6.3 Time Delay Induced into the Real-Time System	36
CHAPTER 7: Implementation	38
7.1 Overview	38
7.2 Implementation in the Test System	38
7.3 Numerical Results of the Proposed Approach	39
7.4 Comparison of $\omega$ and $I_a$ -Based Proposed Approach with $\omega$ -Based Existing Approach	43
7.5 Case Studies	48
7.5.1 Case 1: Real-Time System	48
7.5.2 Case 2: Mechanical Transient Response in a Real-Time System	49
7.5.3 Case 3: Speed control in a Real-time system	50
CHAPTER 8: Conclusion	53
8.1 Conclusion and Summary of Contributions	53
8.2 Future Work	54
REFERENCES	55
APPENDIX A: Matlab Code and Matlab Simulink Model	57
A.1 MATLAB Code	57
A.2 Optimization Strategy	58
APPENDIX B: Notations	61

## LIST OF TABLES

TABLE 7.1: Analysis: ISE of $\omega$	46
TABLE 7.2: Analysis: ISE of $I_a$	47
TABLE 7.3: Analysis: ISE of the Performance Index	48

## LIST OF FIGURES

FIGURE 3.1:	Basic Elementary Feedback System	14
FIGURE 3.2:	Sensitivity points of the feedforward and feedback path	15
FIGURE 3.3:	Measurements of Sensitivity coefficients	15
FIGURE 3.4:	Block diagram of Multiloop System	16
FIGURE 3.5:	Reduced form of the block diagram	17
FIGURE 3.6:	Sensitivity Model	19
FIGURE 4.1:	Separately Excited DC Motor	22
FIGURE 4.2:	Mathematical Model	23
FIGURE 4.3:	Mathematical Model	24
FIGURE 4.4:	Mathematical Model	24
FIGURE 5.1:	Sensitivity Model	27
FIGURE 5.2:	Optimization Block	30
FIGURE 6.1:	Optimization Strategy	32
FIGURE 6.2:	Delayed Input	37
FIGURE 7.1:	Delayed Input	39
FIGURE 7.2:	Sensitivity coefficients $V_1, V_3, V_2, V_4$ for gains $K_1, K_2, K_c, K_s$	40
FIGURE 7.3:	Gradient components $dK_1, dK_2, dK_c, dK_s$ for gains $K_1, K_2, K_c, K_s$	41
FIGURE 7.4:	Updated parameter signals for gains $K_1, K_2, K_c, K_s$	42
FIGURE 7.5:	Initial Motor Response	43
FIGURE 7.6:	Initial Motor Response	43
FIGURE 7.7:	Comparison of optimization results	44
FIGURE 7.8:	Comparison of Approaches: ISE of $\omega$ only	45
FIGURE 7.9:	Comparison of Approaches: ISE of $I_a$ considered separately	46
FIGURE 7.10:	Comparison of Approaches: ISE of the Performance Index	47



FIGURE 7.11: Comparison of Approaches: Real-Time System Output of $\omega$ and $I_a$	49
FIGURE 7.12: Comparison of Approaches: Transient Response of $\omega$ and $I_a$	50
FIGURE 7.13: Comparison of Approaches: Response of $\omega$ and $I_a$ to speed variation	51
FIGURE A.1: Optimisation Strategy	58
FIGURE A.2: Sensitivity Model	59
FIGURE A.3: Gradient Component Calculation	60
FIGURE A.4: Parameter Update	60

## CHAPTER 1: Thesis Organization

### 1.1 Overview

A separately excited DC motor is a motor with separate control for armature and field winding which makes it easier to vary one without influencing the other directly. These motors are widely used for speed varying operations by using 2 methods, field weakening and armature voltage control. In field weakening, the field current is decreased to vary speed of the motor. In armature control, armature voltage is varied. In this study, field control is used by maintaining a constant voltage source to keep the field current constant and hence the angular speed constant. The motor operates in constant power region [13].

There are many methods to tune the parameters of a DC motor drive nowadays. Using neural networks, controllers have been designed to achieve minimum steady state error. The issue with neural network is it is complex and takes time to train the network. There are different algorithms that search for the best set of values of a system. Particle Swarm Optimization is a widely used algorithm that follows neighborhood topology [1]. The value of one particle has influence on its neighbors and the values are updated accordingly. Though, this algorithm has a high computation speed, it has the disadvantage of falling in the local optimum of a population and has a low convergence rate in iterative processes.

In industrial situations, Fuzzy Logic controllers are useful when mathematical model of a process is not known [3]. Fuzzy Logic Controllers can control the system and accommodate the functions of PID controllers. With the mathematical model known, non-fuzzy methods perform better compared to intuitive fuzzy logic [6].

Genetic algorithms are evolutionary algorithms that use a heuristic approach when

the information of a system is unknown. It typically consists of a population of parameters with each parameter used in the next iteration if indicating a favorable variation depending on the fitness function. They are used for obtaining multiple solutions from a system. Hence they are suitable for parallel implementation. GA has the disadvantage of randomness and hence has slow convergence [5].

For systems with mathematical model accurately known, using conventional control methods yields accurate results in a short time [6][7]. In this thesis, the actual parameter values are used and is not done using a stochastic approach. The optimization method in this work uses sensitivity analysis that takes the sensitivity coefficients of the parameters with respect to the output and based on gradient method finds the optimal value [13]. The PID controller is tuned with the optimal values. This method is less explored and can be applied in industrial control. It also has a good convergence rate. Also, the existing research was lacking the quality of dynamic control when compared with other known control approaches [13]. Hence, it provides the scope of improvement. Present research dives in depth of the approach with an aim of improving the quality of dynamic control of DC motor.

## 1.2 Objective

The purpose of this thesis is optimizing the parameter values in a DC motor drive system with respect to the state variables angular velocity  $\omega$  and armature current  $I_a$ . The values so calculated are updated in the parameters of the real-time system to improve the dynamic response by mitigating the initial oscillations in the system. The Integral Squared Error obtained from this approach is analyzed to quantify the improvement in the response of the system. The optimization strategy is implemented for changes in dynamics of the operating condition like excitation, transient and speed variation.

### 1.3 Introduction: Chapters

The optimization strategy is divided into 6 chapters, chapters 2 through chapter 7. They are explained in a compact form below for the reader's convenience.

In chapter 2, the criterion employed for the minimization of error for  $s$  number of state variables is discussed [13][15]. The error in the case is the difference between the actual motor response and the desired motor response. The error is minimized by calculating the performance index  $J(q, q_r)$  and gradient components of the performance index  $\frac{\partial J}{\partial q_j}$ . The formulation of equation for the calculation of performance index values for 3 state variables is given in matrix form.

In chapter 3, the method for analyzing sensitivity of parameters of a system is discussed [12]. The procedure development to determine the sensitivity points and sensitivity functions and calculate sensitivity coefficients is explained for a basic elementary system and also for a multiloop system.

In chapter 4, sensitivity analysis is applied to the mathematical model of a DC Motor Drive [13]. The sensitivity model is developed from the mathematical model to easily locate the sensitivity points. The sensitivity functions of the parameters  $K_1, K_2, K_c, K_s$  considered are calculated. The product of sensitivity points and the function gives the values of sensitivity coefficients for each parameter considered in the system. Here, the concept of parameter update model is shown graphically, briefly explaining how the parameter values are updated over a course of iterations to reach their optimal values.

In chapter 5, the DC motor drive system [11] applied to the sensitivity based parameter optimization is discussed. The system consists of a separately excited DC motor and speed and current controllers respectively. The equations governing the behavior of the system and also their representation in a feedback loop control system is explained. The block diagram reduction is shown in this chapter to obtain a suitable form to develop sensitivity model [12].

In Chapter 6, the Optimization strategy in real-time is discussed. It shows the interaction between the optimization strategy used to find optimal values of the parameters and how these values can improve the dynamic response of the system in a real-time system. It gives a detail on the tolerance for the state variables and the weighing factors used to compare angular velocity and armature current on a common scale. A delayed step function is applied as an input to the actual real-time DC motor system which is waiting for the optimized parameter values from the offline Optimization process and runs with the optimal parameter values when obtained.

In chapter 7, the strategy discussed in the earlier chapters is applied in a test system. The waveforms for sensitivity coefficients of the parameters  $K_1, K_2, K_c, K_s$ , their gradient components with respect to  $\omega$  and  $I_a$ , gain updates and system response for the selected iterations are displayed and explained elaborately. The comparisons made between the results of the prior approach [13] and the proposed approach demonstrates the improvement in the dynamic response of the system. This optimization process is implemented for different cases of dynamic changes in the system. It is implemented for mechanical load transient and for speed variations in the drive system. From the waveforms, it is evident that oscillations are mitigated effectively.

In chapter 8, the results from the test system are analyzed and discussed. It also extends an idea on how the proposed approach can be applied to a non-linear system.

## CHAPTER 2: CONCEPT OF PARAMETER OPTIMISATION APPLIED IN THIS STUDY

### 2.1 Overview

This chapter discusses how to optimize parameters of the system by obtaining their gradient values. A criterion is used to calculate these gradients. The factors that determine the criterion and also the calculation of gradients are given in the following sections.

### 2.2 Criterion

Criterion for the parameter optimization of the dynamic system considered is the difference or mismatch between the reference system response or desired system response and the actual system response, and the error between actual armature current and armature reference current. If the behavior of the system is described by the output of the system for a specific input system excitation, then the criterion is chosen as the integral of the quadratic form of the error between system response and reference model with desired system response.

In the time interval  $[t_0, t_0 + T]$  [13,15], performance index is given by:

$$J = \int_{t_0}^{t_0+T} (\bar{y}(t, \bar{q}) - \bar{y}_r(t))^T Q (\bar{y}(t, \bar{q}) - \bar{y}_r(t)) dt \quad (2.1)$$

where

$$\bar{y}(t, \bar{q}) = [y_i(t, q)]_{s \times 1} = \begin{bmatrix} y_1(t, \bar{q}) \\ y_2(t, \bar{q}) \\ \vdots \\ y_s(t, \bar{q}) \end{bmatrix} : \text{system output vector}$$

$$\bar{y}_r(t) = [y_{ri}(t)]_{s \times 1} = \begin{bmatrix} y_{r1}(t, \bar{q}) \\ y_{r2}(t, \bar{q}) \\ \vdots \\ y_{rs}(t, \bar{q}) \end{bmatrix} : \text{reference model vector}$$

$$Q = [Q_{ii}]_{s \times s} = \begin{bmatrix} Q_{11} & 0 & 0 \\ 0 & Q_{22} & 0 \\ 0 & 0 & \ddots \cdot Q_{ss} \end{bmatrix} : \text{positive definite matrix}$$

$T$  : interval in which we consider system dynamics

The system output vector  $\bar{y}(t, \bar{q})$  is the system response to the applied input. Step function is used for exciting the system.

The desired system output vector  $\bar{y}_r(t)$  is a vector compared with the output of the actual system, in fact it is the ideal output of the system. The length of the time interval  $T$ , should be chosen long enough to cover the time of the system dynamics. If the system dynamics caused by the system excitation, step function  $h(t - t_0)$  is considered,  $T$  may be very long. But practically  $T$  is chosen as the value after which error between reference and actual system output is minimal.

Criterion given by the equation 2.1 depends on the output of the dynamic system, the output of the reference system and the weighting matrix  $Q$ .

$$J = J(\bar{q}, \bar{q}_r) \tag{2.2}$$

where

$$\bar{q} = [q_j]_{m \times 1} = \begin{bmatrix} q_1 \\ q_2 \\ \vdots \\ q_m \end{bmatrix} : \text{system parameters}$$

Here  $\bar{q}$  is the vector.

The problem of minimization of the criterion 2.1 is to determine  $\bar{q}$  such that integral of the square error between the system output and reference model is the minimum.

### 2.3 Optimality Conditions

The first derivative of the performance index with respect to the system parameters set to zero, if satisfied, defines the minimum of the index [13, 14, 15].

$$\frac{\partial J}{\partial q_j} = 0 \quad j=1, 2, \dots, m$$

or

$$\text{grad}J = 0 \quad (2.3)$$

where

$$\text{grad}J = \left[ \frac{\partial J}{\partial q_1}, \frac{\partial J}{\partial q_2}, \dots, \frac{\partial J}{\partial q_m} \right]$$

The equation for gradient component of the performance index is:

$$\frac{\partial J}{\partial q_j} = \int_{t_0}^{t_0+T} \left\{ \left[ \frac{\partial \bar{y}(t, \bar{q})}{\partial q_j} \right]^T Q (\bar{y}(t, \bar{q}) - \bar{y}_r(t)) + (\bar{y}(t, \bar{q}) - \bar{y}_r(t))^T Q \frac{\partial \bar{y}(t, \bar{q})}{\partial q_j} \right\} dt \quad (2.4)$$

As an example let's look at the system with 3 state variables and 3 system outputs.

Assume that the system has 3 parameters that can be changed.

In expanded form, gradient component of the performance index in vector form is

$$\frac{\partial J}{\partial q_j} = \int_{t_0}^{t_0+T} \left\{ \begin{bmatrix} \frac{\partial y_1(t, \bar{q})}{\partial q_j} \\ \frac{\partial y_2(t, \bar{q})}{\partial q_j} \\ \frac{\partial y_3(t, \bar{q})}{\partial q_j} \end{bmatrix} \begin{bmatrix} Q_{11} & 0 & 0 \\ 0 & Q_{22} & 0 \\ 0 & 0 & Q_{33} \end{bmatrix} \begin{bmatrix} y_1(t, \bar{q}) - y_{r1}(t) \\ y_2(t, \bar{q}) - y_{r2}(t) \\ y_3(t, \bar{q}) - y_{r3}(t) \end{bmatrix} \right\} \quad j = 1, 2, 3$$



$$\begin{aligned}
& + \left[ \begin{array}{ccc} y_1(t, \bar{q}) - y_{r1}(t) & y_2(t, \bar{q}) - y_{r2}(t) & y_3(t, \bar{q}) - y_{r3}(t) \end{array} \right] \\
& \left[ \begin{array}{ccc} Q_{11} & 0 & 0 \\ 0 & Q_{22} & 0 \\ 0 & 0 & Q_{33} \end{array} \right] \left[ \begin{array}{c} \frac{\partial y_1(t, \bar{q})}{\partial q_j} \\ \frac{\partial y_2(t, \bar{q})}{\partial q_j} \\ \frac{\partial y_3(t, \bar{q})}{\partial q_j} \end{array} \right] \} dt \quad (2.5)
\end{aligned}$$

or multiplying expressions, gradient components are of the form

$$\begin{aligned}
\frac{\partial J}{\partial q_j} &= \int_{t_0}^{t_0+T} \left\{ \begin{array}{ccc} \frac{\partial y_1(t, \bar{q})}{\partial q_j} Q_{11} & \frac{\partial y_2(t, \bar{q})}{\partial q_j} Q_{22} & \frac{\partial y_3(t, \bar{q})}{\partial q_j} Q_{33} \end{array} \right\} \left[ \begin{array}{c} y_1(t, \bar{q}) - y_{r1}(t) \\ y_2(t, \bar{q}) - y_{r2}(t) \\ y_3(t, \bar{q}) - y_{r3}(t) \end{array} \right] \\
& + \left[ \begin{array}{ccc} y_1(t, \bar{q}) - y_{r1}(t) & y_2(t, \bar{q}) - y_{r2}(t) & y_3(t, \bar{q}) - y_{r3}(t) \end{array} \right] \left[ \begin{array}{c} \frac{\partial y_1(t, \bar{q})}{\partial q_j} Q_{11} \\ \frac{\partial y_2(t, \bar{q})}{\partial q_j} Q_{22} \\ \frac{\partial y_3(t, \bar{q})}{\partial q_j} Q_{33} \end{array} \right] \} dt
\end{aligned}$$

$$\begin{aligned}
\frac{\partial J}{\partial q_j} &= 2 \left[ \frac{\partial y_1(t, \bar{q})}{\partial q_j} Q_{11} (y_1(t, \bar{q}) - y_{r1}(t)) + \frac{\partial y_2(t, \bar{q})}{\partial q_j} Q_{22} (y_2(t, \bar{q}) - y_{r2}(t)) \right. \\
& \left. + \frac{\partial y_3(t, \bar{q})}{\partial q_j} Q_{33} (y_3(t, \bar{q}) - y_{r3}(t)) \right] dt
\end{aligned}$$

$$\frac{\partial J}{\partial q_j} = \int_{t_0}^{t_0+T} \left[ \begin{array}{ccc} (y_1(t, \bar{q}) - y_{r1}(t)) & (y_2(t, \bar{q}) - y_{r2}(t)) & (y_3(t, \bar{q}) - y_{r3}(t)) \end{array} \right] \left[ \begin{array}{c} 2 \frac{\partial y_1(t, \bar{q})}{\partial q_j} Q_{11} \\ 2 \frac{\partial y_2(t, \bar{q})}{\partial q_j} Q_{22} \\ 2 \frac{\partial y_3(t, \bar{q})}{\partial q_j} Q_{33} \end{array} \right] dt$$

$$\frac{\partial J}{\partial q_j} = \int_{t_0}^{t_0+T} \left\{ \begin{bmatrix} (y_1(t, \bar{q}) - y_{r1}(t)) & (y_2(t, \bar{q}) - y_{r2}(t)) & (y_3(t, \bar{q}) - y_{r3}(t)) \end{bmatrix} \right. \\ \left. \left[ \begin{bmatrix} Q_{11} & 0 & 0 \\ 0 & Q_{22} & 0 \\ 0 & 0 & Q_{33} \end{bmatrix} + \begin{bmatrix} Q_{11} & 0 & 0 \\ 0 & Q_{22} & 0 \\ 0 & 0 & Q_{33} \end{bmatrix}^T \right] \begin{bmatrix} \frac{\partial y_1(t, \bar{q})}{\partial q_j} \\ \frac{\partial y_2(t, \bar{q})}{\partial q_j} \\ \frac{\partial y_3(t, \bar{q})}{\partial q_j} \end{bmatrix} \right\} dt$$

and finally,

$$\frac{\partial J}{\partial q_j} = \int_{t_0}^{t_0+T} \left\{ \begin{bmatrix} (y_1(t, \bar{q}) - y_{r1}(t)) & (y_2(t, \bar{q}) - y_{r2}(t)) & (y_3(t, \bar{q}) - y_{r3}(t)) \end{bmatrix} \right. \\ \left. \left[ \begin{bmatrix} Q_{11} & 0 & 0 \\ 0 & Q_{22} & 0 \\ 0 & 0 & Q_{33} \end{bmatrix} + \begin{bmatrix} Q_{11} & 0 & 0 \\ 0 & Q_{22} & 0 \\ 0 & 0 & Q_{33} \end{bmatrix}^T \right] \begin{bmatrix} U_1 \\ U_2 \\ U_3 \end{bmatrix} \right\} dt$$

Here  $U_1, U_2, U_3$  are partial derivatives of the three outputs with  $q_j$  parameters,  $j=1, 2, 3, 4$ .

or

$$\bar{U}_{ij}(t, \bar{q}) = \left[ \frac{\partial y_i(t, \bar{q})}{\partial q_j} \right]$$

where  $\bar{U}_{ij}(t, \bar{q})$  [12] is the sensitivity function of the system with respect to the  $q_j$  parameters.

If the system has  $i$  state variables and  $j$  number of parameters, the performance index gradient would be in matrix form.

$$\frac{\partial J}{\partial \bar{q}} = \int_{t_0}^{t_0+T} \left\{ [y_1(t, \bar{q}) - \bar{y}_r(t)]^T [[Q] + [Q]^T] \left[ \frac{\partial y(t, \bar{q})}{\partial \bar{q}} \right] \right\} dt \quad (2.6)$$

$$\frac{\partial J}{\partial \bar{q}} = \int_{t_0}^{t_0+T} \left\{ [y_1(t, \bar{q}) - \bar{y}_r(t)]^T [[Q] + [Q]^T] [U(t, \bar{q})] \right\} dt \quad (2.7)$$

Therefore, to determine the conditions for the optimality i.e., gradient  $J$ , it is necessary to determine sensitivity coefficients for system parameters with respect to the state variables being optimized. If the system with only one input with system's initial values equal to zero is considered, the sensitivity functions can be relatively easily calculated.

Consider 2 state variables, the angular velocity  $\omega$  and  $I_a$ . In this study, the system considered is the DC motor drive. Four parameters considered in this study are the gains. Notation for these parameters are  $K_1, K_2, K_c, K_s$ . The parameters  $q_j$ ,  $j = 1, 2, 3, 4$  are identified in the motor drive system as the gains  $K_1, K_2, K_c, K_s$ . The gradient vector is with notation

$$\text{grad}J = \left[ \frac{\partial J}{\partial K_1} \frac{\partial J}{\partial K_2} \frac{\partial J}{\partial K_c} \frac{\partial J}{\partial K_s} \right]$$

For a function,  $J = \int_{t_0}^{t_0+T} [\bar{y}(t, \bar{q}) - \bar{y}_r(t)]^T Q [\bar{y}(t, q) - \bar{y}_r(t)] dt$ , criterion with respect to  $\omega$  is:

$$\frac{\partial J_1}{\partial K_1} = \int_{t_0}^{t_0+T} \{ [y_1(t, K_1) - y_{r1}(t)]^T [[Q] + [Q]^T] \left[ \frac{\partial y_1(t, K_1)}{\partial K_1} \right] \} dt$$

$$\frac{\partial J_1}{\partial K_2} = \int_{t_0}^{t_0+T} \{ [y_1(t, K_2) - y_{r1}(t)]^T [[Q] + [Q]^T] \left[ \frac{\partial y_1(t, K_2)}{\partial K_2} \right] \} dt$$

$$\frac{\partial J_1}{\partial K_c} = \int_{t_0}^{t_0+T} \{ [y_1(t, K_c) - y_{r1}(t)]^T [[Q] + [Q]^T] \left[ \frac{\partial y_1(t, K_c)}{\partial K_c} \right] \} dt$$

$$\frac{\partial J_1}{\partial K_s} = \int_{t_0}^{t_0+T} \{ [y_1(t, K_s) - y_{r1}(t)]^T [[Q] + [Q]^T] \left[ \frac{\partial y_1(t, K_s)}{\partial K_s} \right] \} dt$$

or

$$\frac{\partial J_1}{\partial \bar{q}} = \int_{t_0}^{t_0+T} \{ [y_2(t, \bar{q}) - \bar{y}_{r2}(t)]^T [[Q] + [Q]^T] \left[ \frac{\partial y_1(t, \bar{q})}{\partial K_1} \quad \frac{\partial y_1(t, \bar{q})}{\partial K_2} \quad \frac{\partial y_1(t, \bar{q})}{\partial K_c} \quad \frac{\partial y_1(t, \bar{q})}{\partial K_s} \right] \} dt \quad (2.8)$$

Criterion with respect to armature current  $I_a$ :

$$\frac{\partial J_2}{\partial K_1} = \int_{t_0}^{t_0+T} \{ [y_2(t, K_1) - y_{r2}(t)]^T [[Q] + [Q]^T] \left[ \frac{\partial y_2(t, K_1)}{\partial K_1} \right] \} dt$$

$$\frac{\partial J_2}{\partial K_2} = \int_{t_0}^{t_0+T} \{ [y_2(t, K_2) - y_{r2}(t)]^T [[Q] + [Q]^T] \left[ \frac{\partial y_2(t, K_2)}{\partial K_2} \right] \} dt$$

$$\frac{\partial J_2}{\partial K_c} = \int_{t_0}^{t_0+T} \{ [y_2(t, K_c) - y_{r2}(t)]^T [[Q] + [Q]^T] \left[ \frac{\partial y_2(t, K_c)}{\partial K_c} \right] \} dt$$

$$\frac{\partial J_2}{\partial K_s} = \int_{t_0}^{t_0+T} \{ [y_2(t, K_s) - y_{r2}(t)]^T [[Q] + [Q]^T] \left[ \frac{\partial y_2(t, K_s)}{\partial K_s} \right] \} dt$$

or

$$\frac{\partial J_2}{\partial \bar{q}} = \int_{t_0}^{t_0+T} \{ [y_2(t, \bar{q}) - \bar{y}_{r2}(t)]^T [[Q] + [Q]^T] \left[ \frac{\partial y_2(t, \bar{q})}{\partial K_1} \quad \frac{\partial y_2(t, \bar{q})}{\partial K_2} \quad \frac{\partial y_2(t, \bar{q})}{\partial K_c} \quad \frac{\partial y_2(t, \bar{q})}{\partial K_s} \right] \} dt \quad (2.9)$$

In the next chapter 3, calculations of the system sensitivities  $U_{1j}$  and performance index gradient components are shown.

#### 2.4 Minimization of the criterion with multiple parameters

There are a number of iterative methods used for this purpose. All the methods have developed algorithms which based on initial parameters selected  $\bar{q}^0$ , in an iterative procedure calculate the parameters which are further moving the criterion to its minimum. In k iterations, we calculate  $\bar{q}^0, \bar{q}^1, \dots, \bar{q}^k$  parameters are calculated where k is the last computed iteration which gives the minimum of the criterion [13].

$$\lim_{k \rightarrow \infty} \bar{q}^k = \bar{q}_{min} \quad (2.10)$$

where K is the number of iterations.

$$gradJ(\bar{q}_{min}) \simeq 0 \quad (2.11)$$

The iterations stop when the dynamic response of the system reaches its set tolerance value. The value of the parameters then obtained are the optimal values, that are applied to improve the dynamic response of the real-time system.

In the following chapter, sensitivity analysis of parameters in a basic elementary control system is given and is further developed for complex multiloop control systems.

## CHAPTER 3: SENSITIVITY ANALYSIS

### 3.1 Overview

The concept of sensitivity analysis is introduced here for elementary control systems and is further developed for multi-loop control systems. The sensitivity functions for both feedforward and feedback loops are defined in this chapter.

### 3.2 Elementary System Analysis

The theory is fully presented in [12] where the method for evaluating the sensitivity coefficients is developed for an elementary linear system with two parameters. The method is not widely known and it is presented here to make it easier to follow the development of the sensitivity model for this case study. The procedure enables us to inquire sensitivity points in the system at which sensitivity signals of the parameters under consideration can be picked. Sensitivity coefficients are obtained from the model block diagram as the product of sensitivity signals and sensitivity functions.

### 3.3 The Procedure Development

Consider a system with a transfer function  $W(s_1q_1, \dots, q_m)$ . The transfer function depends on the  $m$  parameters  $q_1, q_2, \dots, q_m$ . The relation between the input and the output of the system is represented as follows:

$$X(s, q_1 \dots, q_m) = Y(s)W(s, q_1 \dots, q_m) \quad (3.1)$$

where  $X(s_1, q_1, \dots, q_m)$  is response for the system to the input, as we apply unit step function  $Y(s)$ .

The sensitivity function  $V_r(s)$  is defined as partial derivative of the output with

respect to the relative parameter [12].

$$V_r = \frac{\partial X(s, q_1 \cdots, q_m)}{\partial \ln q_r} \quad (3.2)$$

Consider a basic feedback system. The feedforward path and feedback path has  $q_1$  and  $q_2$  parameters as their gains respectively. The transfer functions are  $W_1(s)$  and  $W_2(s)$  and are independent of the parameters. The closed-loop transfer function of the system is

$$W(s, q_1, q_2) = \frac{q_1 W_1(s)}{1 + q_1 W_1(s) W_2(s)} \quad (3.3)$$

where this function is relative to the variation in parameter  $q_r$ . The sensitivity function represented in the Laplace transform and the block diagram are given in Fig3.1 [12]. The sensitivity function in time domain can be determined by taking inverse Laplace transform.

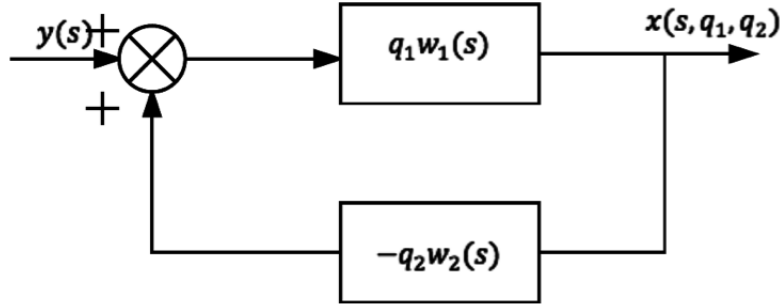


Figure 3.1: Basic Elementary Feedback System.

From equations 3.1 & 3.2 and the block diagram we get the sensitivity coefficients, at the points  $S_1$  and  $S_2$  [12]

$$V_1(s) = X(s) \frac{1}{1 + q_1 W_1(s) W_2(s)} \quad (3.4)$$

$$V_2(s) = X(s) \frac{-q_1 W_1(s) W_2(s)}{1 + q_1 W_1(s) W_2(s)}$$

To understand how sensitivity functions are calculated, consider the block diagram given in Fig 3.1.

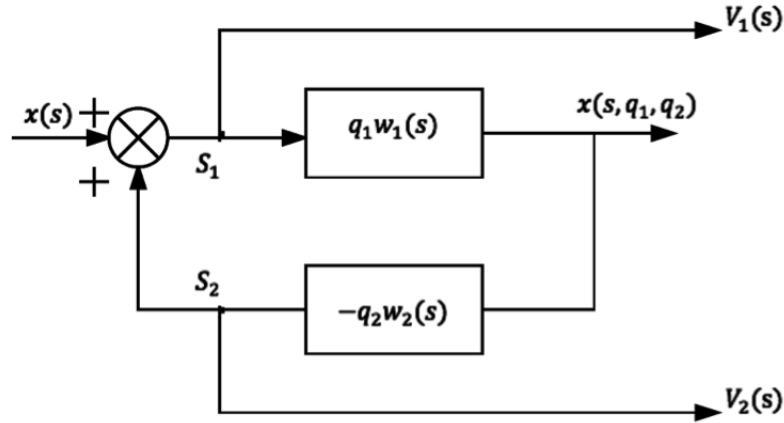


Figure 3.2: Sensitivity points of the feedforward and feedback path.

Sensitivity points are created as  $S_1$  and as  $S_2$  when input is applied in the sensitivity model. The sensitivity coefficient for each parameter  $V_1(s)$  and  $V_2(s)$  can be observed through these points.

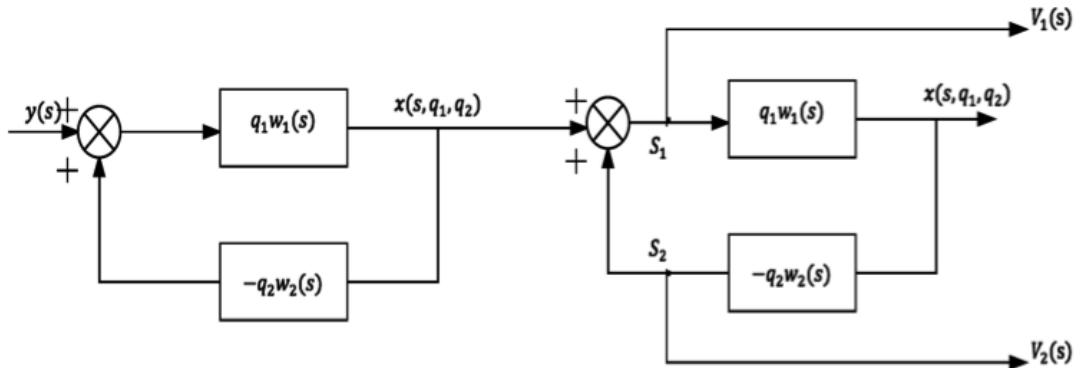


Figure 3.3: Measurements of Sensitivity coefficients.

There are two ways in which we can supply input  $X(s)$  to the sensitivity model. One method is by obtaining output from a generated mathematical model of the system. The other method is to generate the output of the actual system working in



real-time.

Consider the general case with multiple forward and feedback path with each transfer function block and one parameter in each of the blocks. Fig 3.4 [12][13] is a block diagram of the system with  $m$  parameters and a multiloop system structure. It may be noted that the number of sensitivity points depends on the number of parameters, and the number of feedback blocks.

### 3.4 The Analysis of a Multiloop Structure

The method of finding sensitivity coefficients for a basic feedback system was discussed in the earlier section for two parameters only. For a multiloop system, the sensitivity coefficients are obtained from the system block diagram based on an analysis of  $m$  parameters [12].

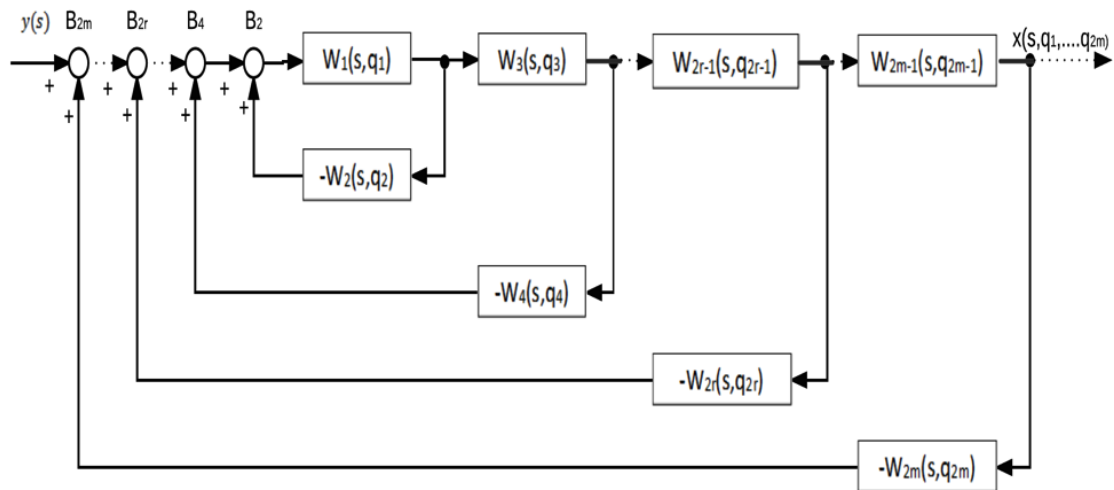


Figure 3.4: Block diagram of Multiloop System.

The model consists of  $2m$  blocks. The transfer functions in the forward and feedback block are  $W_{2r-1}(s, q_{2r-1})$  and  $W_{2r}(s, q_{2r})$  respectively. Let's assume that

there is only one parameter in each of the transfer function. All parameters from  $q_{2r-1}$  to  $q_{2r}$ , where  $r$  is the parameter for which the sensitivity coefficient is calculated. The coefficients  $V_{2r-1}$  to  $V_{2r}$  are the coefficients calculated for  $q_{2r-1}$  to  $q_{2r}$  respectively. This block diagram given maybe reduced to a compact form as shown in Fig 3.5 [12].

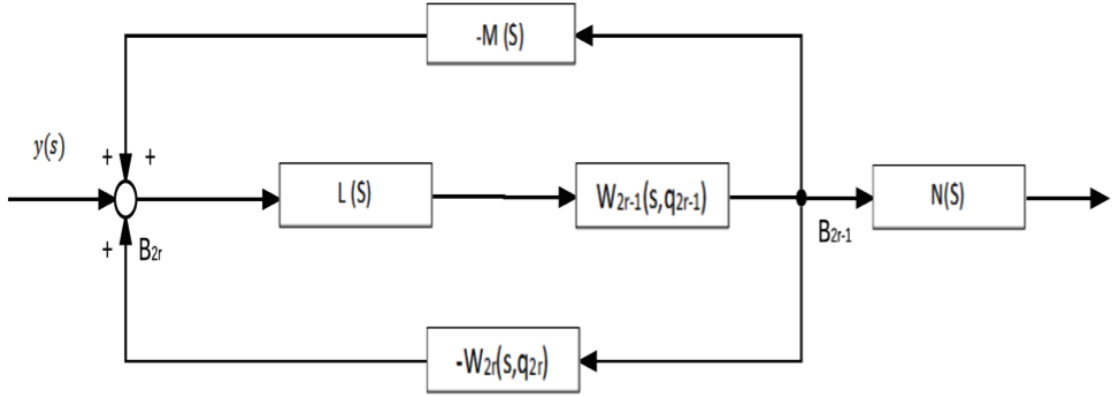


Figure 3.5: Reduced form of the block diagram.

where  $L(s)$  is closed loop transfer function between  $B_{2r-2}$  and  $B_{2r-3}$ .  $M(s)$  and  $N(s)$  are transfer functions given as [12]:

$$M(s) = \sum_{i=r+1}^m W_{2i-1}(s)W_{2i}(s) \quad (3.5)$$

$$N(s) = \prod_{i=r}^m W_{2i}(s)$$

and  $F(s) = M(s) + W_{2r}(s, q_{2r})$

The  $X(s, q_{r-1})$  the is

$$X(s, q_{2r-1}) = Y(s)N(s) \frac{L(s)W_{2r-1}(s, q_{2r-1})}{1 + L(s)W_{2r-1}(s, q_{2r-1})} \quad (3.6)$$

Using the above equation,  $V_{2r-1}(s)$  is calculated

$$V_{2r-1}(s) = X(s) \frac{1}{1 + L(s)F(s)W_{2r-1}(s, q_{2r-1})} \frac{q_{2r-1}}{W_{2r-1}(s, q_{2r-1})} \frac{\partial W_{2r-1}(s, q_{2r-1})}{\partial q_{2r-1}} \quad (3.7)$$

Now, to find the complex sensitivity coefficient  $V_{2r}$ , keep the feedback path  $W_{2r}(s, q_{2r})$  and replace the blocks between  $B_{2r}$  and  $B_{2r-1}$  by the closed loop transfer function.

$$G(s) = \frac{L(s)W_{2r-1}(s)}{1 + L(s)M(s)W_{2r-1}(s)} \quad (3.8)$$

such that

$$X(s, q_{2r-1}) = Y(s)N(s) \frac{G(s)}{1 + G(s)W_{2r}(s, q_{2r})} \quad (3.9)$$

we get for  $V_{2r}$

$$V_{2r}(s) = X(s) \frac{-W_{2r}(s, q_{2r})G(s)}{1 + G(s)W_{2r}(s, q_{2r})} \frac{q_{2r}}{W_{2r}(s, q_{2r})} \frac{\partial W_{2r}(s, q_{2r})}{\partial q_{2r}} \quad (3.10)$$

These equations represent the product of the system response and of the two transfer functions. The first transfer function defines the location of sensitivity point. The second transfer function is the sensitivity transfer function given by

$$T_i(s) = \frac{q_i}{W_i(s, q_i)} \frac{\partial W_i(s)}{\partial q_i} = \frac{\partial \ln W_i(s)}{\partial \ln q_i}; \quad i = 2r - 1, 2r \quad (3.11)$$

In Fig 3.6 [12], we represent block diagram of calculating sensitivity coefficients. The signal  $x(t)$  given as an input is obtained as the output for the system with an input signal  $y(t)$  to the sensitivity model. As we can see, the signals from the sensitivity points  $S_1 \dots, S_{2m}$  feed the sensitivity transfer functions  $T_1(s) \dots, T_{2m}(s)$  so that the sensitivity coefficients  $V_1(s) \dots, V_{2m}(s)$  are obtained as outputs at the end of this calculation.

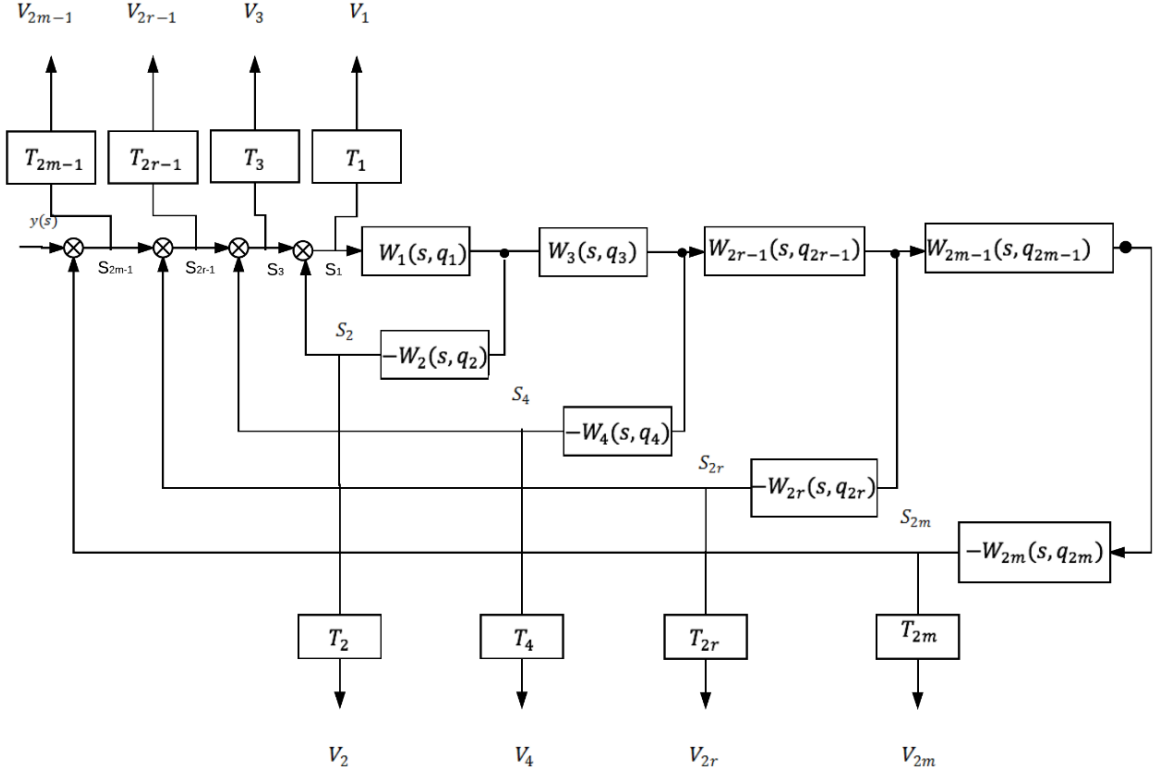


Figure 3.6: Block Diagram of Sensitivity Model of the system with  $2m$  parameters

Generally, all the sensitivity coefficients of different parameters can be obtained simultaneously. The following step is calculation of  $T_i(s)$  for every possible form of the block transfer functions depending on how the parameters are placed in the transfer functions. The parameter for which the sensitivity is analyzed is taken as gain factor of the transfer function.

$$W_j(s, q_i) = q_j G_j(s); \quad j = 2r, 2r - 1 \quad (3.12)$$

$$T_j(s) = \frac{q_j}{q_j G(s)} \frac{\partial q_j G(s)}{\partial q_j} = 1 \quad (3.13)$$

In this case, there is no need to add any more blocks. The sensitivity coefficient is obtained directly as can be noticed. When the elementary transfer function is a product of 2 transfer functions and the sensitivity of only one parameter is to be

analyzed; then

$$W_j(s, q_j) = H_j(s, q_j)D_j(s) \quad (3.14)$$

$$T_j(s) = \frac{q_j}{W_j(s, q_j)} \frac{\partial W_j(s, q_j)}{\partial q_j} = \frac{q_j}{H(s, q_j)} \frac{\partial H(s, q_j)}{\partial q_j} \quad (3.15)$$

The equation 3.15 [12][15] exhibits that the sensitivity coefficient is dependent only on the transfer function containing the parameter being investigated where  $H(s, q_j)$  is the transfer function having the parameter being investigated.

Separately excited DC motor drive system is used in this study is introduced in the next chapter. Behavior of the system and modification of the motor drive control block diagram to form the sensitivity model is shown.

## CHAPTER 4: DC MOTOR DRIVE MODEL

### 4.1 Overview

A separately excited DC motor drive system is used to implement the proposed approach. The equations governing behavior of the system and the assumptions made for the design of the model are given in this chapter. General consideration of the motor drive in this study is based on the references [11, 13].

### 4.2 Structure of the DC Motor Drive with Controllers

The motor drive model is used as known. Under the assumption of small variations around an equilibrium point and arbitrarily chosen reference operating state, DC motor drive model is linearized and described as a set of first order Differential Equation with constant coefficients. For the parameter synthesis of the motor drive, it is important to choose rational structure of the regulators and the values of the regulator parameters in order to obtain high quality of transients and the small steady state error. In simplified analysis, the parameters of the regulators can be chosen on the basis of known relationship between transients and logarithmic AF characteristics of the closed loop system. In that case optimal parameter values are obtained on the basis of adjustment of logarithmic characteristics. In this analysis, thyristor is considered as device without inertia or as device with very small time constant. The thyristor as an element of DC motor drive is non-linear device that has specific qualities affecting the whole transients as much as the bandwidth at the linear part of the system constraining the bandwidth, these effects can be reduced to the very low level. Under these assumptions, thyristor may be considered as a linear device without inertia. These conclusions were studied in [11]. Hybrid diagram of a

separately excited DC motor drive considered in this study is given in Fig. 4.1 [11].

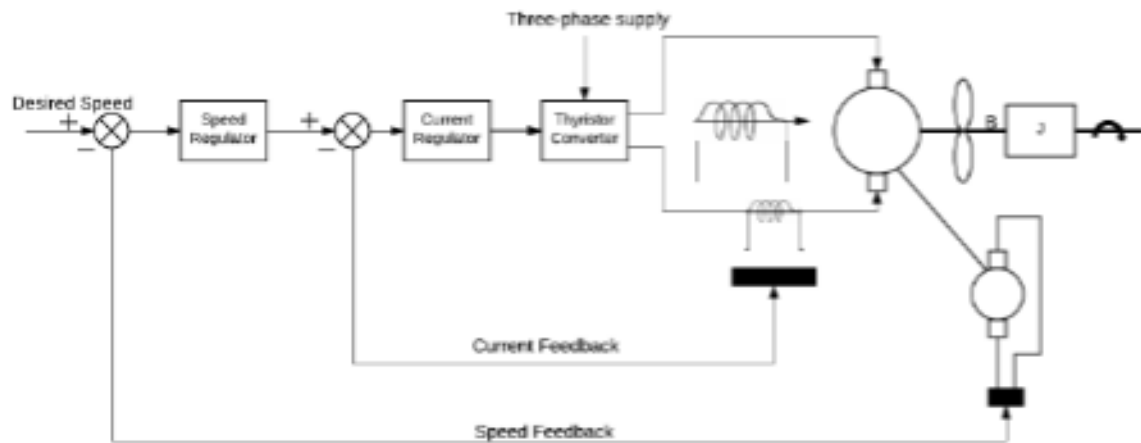


Figure 4.1: Separately Excited DC Motor.

The essential part of the system under this study is the separately excited DC motor supplied through a three-phase full wave thyristor converter. The thyristor conduction angle is controlled so that the ratio of output DC voltage to thyristor command signal is constant. Continuous conduction mode of operation is assumed for converter and any effect of current harmonics to the system are made negligible. Time constant of the thyristor converter is small compared to the time constant of the drive and be ignored without significant error. It is supposed that the field excitation of the motor is constant, although there is no difficulty to include variable excitation in the analysis. The armature reaction is assumed to be negligible so that the motor air gap flux is constant. Control loops are armature current and motor speed. The current and speed regulators are PID type. The transfer functions in the feedback loops are constant. Armature resistance is used as resistance of the armature windings only. Its value can be adjusted to include brush and connecting lead resistances if higher accuracy is desired. Also adjusting resistance  $R$  will include stray load losses. All of these have been presented in the references [13]. Next, the block diagram of the motor drive is presented.

### 4.3 DC Motor Drive Model Functions

The transfer functions of the current and speed regulators are as:

$$W_c(p) = K_2 \frac{T_2 p + 1}{T_2 p} \quad (4.1)$$

$$W_s(p) = K_1 \frac{T_1 p + 1}{T_1 p} \quad (4.2)$$

And the equations describing the motor drive are [11]

$$U_f = R_f I_f$$

$$U_a = \omega C_e + (R_a + L_a p) i_a \quad (4.3)$$

$$T_a = C_e i_a = T_L + \omega(B + Jp)$$

The block diagram is given as:

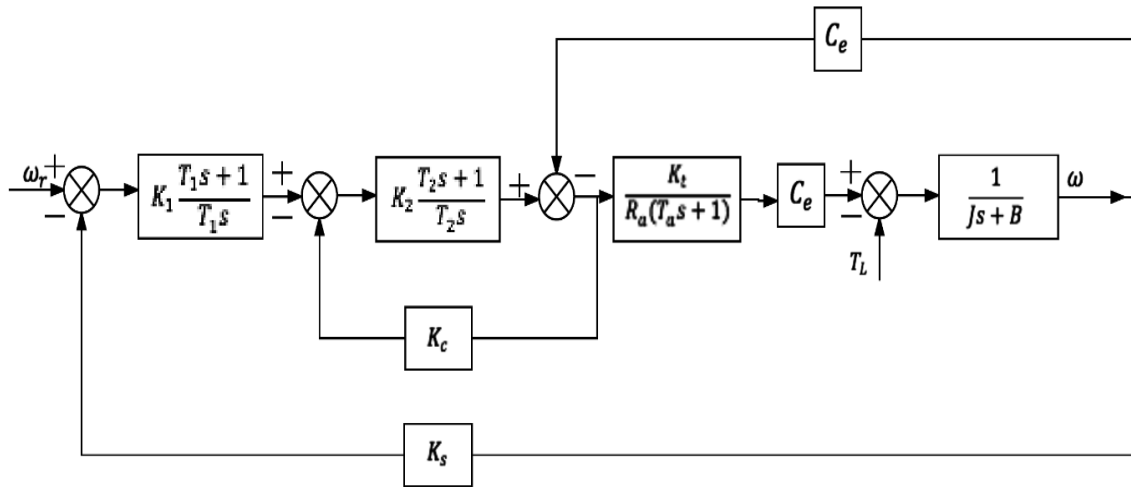


Figure 4.2: DC Motor Block Diagram.

The block diagram in Fig 4.2 can be modified as [8][10]:



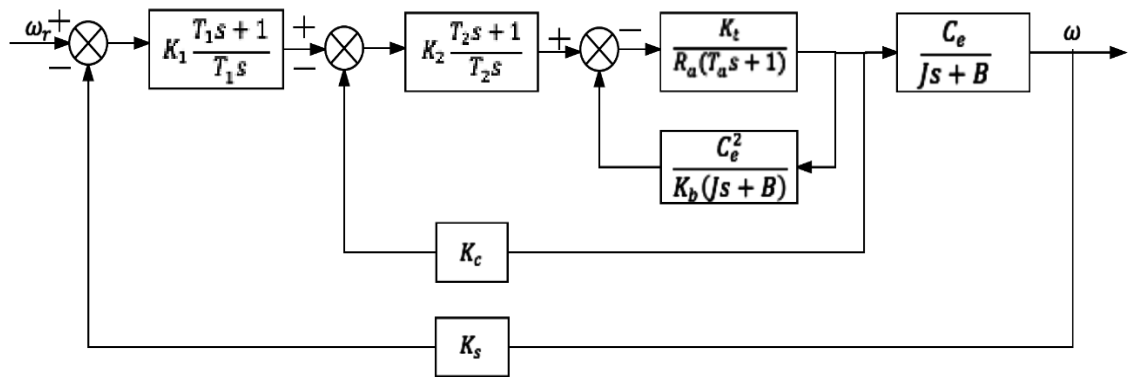


Figure 4.3: Modified Block Diagram.

The sensitivity block diagram for our motor drive required to develop the sensitivity model is obtained in Fig 4.4 [13].

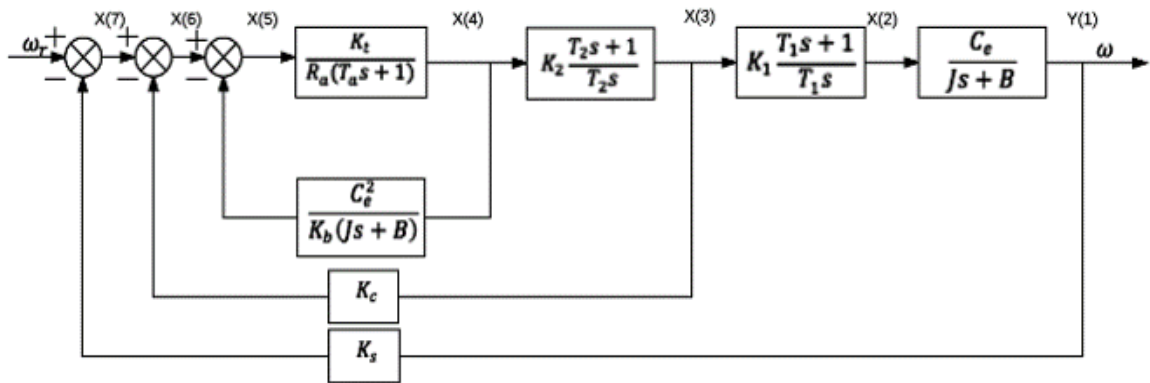


Figure 4.4: Block Diagram modified to develop Sensitivity Model.

The set of differential equations describing the behavior of the system:

$$\frac{dY(1)}{dt} = -\frac{B}{J}Y(1) + \frac{C_e}{J}Y(2)$$

$$\frac{dY(2)}{dt} = \frac{K_1 X(3)}{T_1}$$

$$\begin{aligned}
\frac{dY(3)}{dt} &= \frac{K_2}{T_2}X(4) = \frac{K_2}{T_2}Y(4) \\
\frac{dY(9)}{dt} &= \frac{1}{T_a}[K_a K_t X(5) - Y(4)] \\
\frac{dY(5)}{dt} &= -\frac{C_e^2}{JK_t}Y(4) + \frac{B}{J}Y(5)
\end{aligned} \tag{4.4}$$

where

$$\begin{aligned}
X(7) &= \omega_r - K_s * Y(1) \\
X(3) &= Y(3) + Y(4) * K_2 \\
X(2) &= Y(2) + X(3) * K_1 \\
X(6) &= X(7) - K_c * X(3) \\
X(5) &= Y(5) + X(6)
\end{aligned} \tag{4.5}$$

These differential equations are used to form differential equations of the sensitivity model. In chapter 5, sensitivity model is developed for the drive system. The differential equations of the performance index (PI) is defined for  $\omega$  and  $I_a$  respectively. The equations required to find the gradients of PI with respect to the gains are also defined.

## CHAPTER 5: Sensitivity Model Applied To a Motor Drive System

### 5.1 Overview

The sensitivity model developed is based on the motor drive model. The motor drive model used is developed in the literature references[11,13]. The same motor drive model has been analyzed in different studies from several viewpoints. This study focuses on parameter optimization by criterion minimization, which is defined as the integral squared error of the motor speed and armature current. The output from the mathematical model is applied into the system's sensitivity model as the input. From the modified model, in Fig 4.4, sensitivity points are located and the sensitivity functions are calculated subsequently. Sensitivity functions actually help in determining gradient components of the criterion for each of the parameters in the optimization process. In the iterative process described earlier, performance index is minimized and the optimal parameters are obtained. In this study, the parameters are  $\bar{q}$  with the components  $q_1, q_2 \cdots q_m$ . The motor drive example has 4 gains that are considered for parameter optimization. The gains analyzed are as follows.  $K_1$  is gain of the speed regulator,  $K_2$  is gain of the current regulator,  $K_c$  is gain of the current feedback loop and  $K_s$  is gain of the speed feedback loop.

Sensitivity points at  $j = 1, 2, 3, 4$  are located following the rules developed in the chapter 3 are shown in Fig. 5.1 [13]. Two of them are located before the transfer functions in the forward path and another two are after the transfer functions in the feedback path.

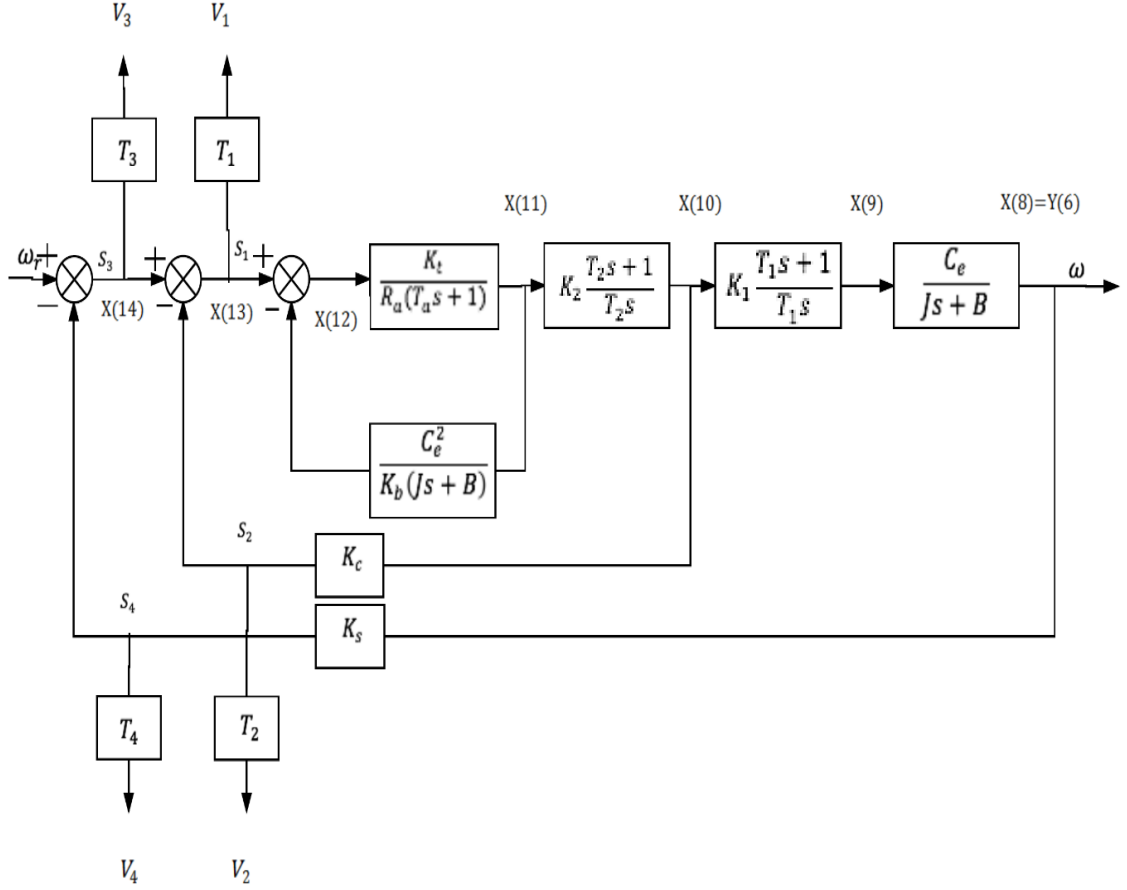


Figure 5.1: Sensitivity Model .

After these sensitivity points, sensitivity functions are calculated to get the gradient of the performance index with respect to the four gains under considerations [12].

$$T_j = \frac{q_j}{W_j(s, q_j)} \frac{\partial}{\partial t} [W_j(s, q_j)]; \quad j = 1, 2, 3, 4 \quad (5.1)$$

All of our parameters considered  $K_1$ ,  $K_2$ ,  $K_c$ ,  $K_s$  are gains.

## 5.2 Mathematical Model

The sensitivity model is represented by five differential equations. Referring to the model the equations are [13]:

$$\frac{dY(6)}{dt} = -\frac{B}{J}Y(6) + \frac{C_e}{J}Y(9)$$

$$\begin{aligned}
\frac{dY(7)}{dt} &= \frac{K_1 X(10)}{T_1} \\
\frac{dY(8)}{dt} &= \frac{K_2}{T_2} X(11) = \frac{K_2}{T_2} Y(9) \\
\frac{dY(9)}{dt} &= \frac{1}{T_a} [K_a K_t X(12) - Y(9)] \\
\frac{dY(10)}{dt} &= -\frac{C_e^2}{J K_t} Y(9) + \frac{B}{J} Y(10)
\end{aligned} \tag{5.2}$$

where

$$\begin{aligned}
X(14) &= Y(1) - K_s * Y(6) \\
X(10) &= Y(8) + Y(9) * K_2 \\
X(9) &= Y(7) + X(10) * K_1 \\
X(13) &= X(14) - K_c * X(10) \\
X(12) &= Y(10) + X(13)
\end{aligned} \tag{5.3}$$

As discussed earlier in this chapter, sensitivity functions are used to minimize performance index. The performance index depends on the variation of the motor speed and armature current[13] respectively and are given by the differential equations:

$$\frac{dJ_1}{dt} = \frac{1}{2} [\omega_r - K_s Y(1)]^2 \tag{5.4}$$

$$\frac{dJ_2}{dt} = \frac{1}{2} [X(7) - K_c X(3)]^2 \tag{5.5}$$

The performance index is minimized using sensitivity functions by means of gradient method. Sensitivity functions are given by [12, 13]:

$$\begin{aligned}
V(1) &= Y(13) & V(2) &= X(14) \\
V(3) &= -K_c * X(10) & V(4) &= -K_s * Y(6)
\end{aligned} \tag{5.6}$$

Y(12) and Y(13) are obtained by solving the following two differential equations

$$\frac{dY(12)}{dt} = -\frac{Y(12) + X(13)}{T_2} \quad (5.7)$$

$$\frac{dY(13)}{dt} = -\frac{Y(13) + X(12)}{T_1} \quad (5.8)$$

To obtain the gradient component of performance index, the following set of differential equations is solved for each parameter

$$\frac{d}{dt}\left(\frac{\partial J_1}{\partial q_j}\right) = \frac{dY(I)}{dt} = \frac{[\omega_r - K_s Y(1)]K_s * V(J)}{q_j} \quad I = 14, 15 \dots 18 \text{ and } j = 1, 2, 3, 4 \quad (5.9)$$

$$\frac{d}{dt}\left(\frac{\partial J_1}{\partial K_s}\right) = \frac{dY(19)}{dt} = [\omega_r - K_s Y(1)] * [Y(1) + V(4)] \quad (5.10)$$

$$\frac{d}{dt}\left(\frac{\partial J_2}{\partial q_j}\right) = \frac{dY(I)}{dt} = \frac{[X(7) - K_c X(3)]K_c * V(J)}{q_j} \quad I = 20, \dots 24 \text{ and } j = 1, 2, 3, 4 \quad (5.11)$$

$$\frac{d}{dt}\left(\frac{\partial J_2}{\partial K_c}\right) = \frac{dY(25)}{dt} = [\omega_r - K_c X(3)] * [X(3) + V(2)] \quad (5.12)$$

All the differential equations obtained here are solved to get sensitivity coefficients, value of performance index and gradients.

### 5.3 Optimization Concept and Block Diagram

In this block diagram, the concept of parameter update based on the theory presented.

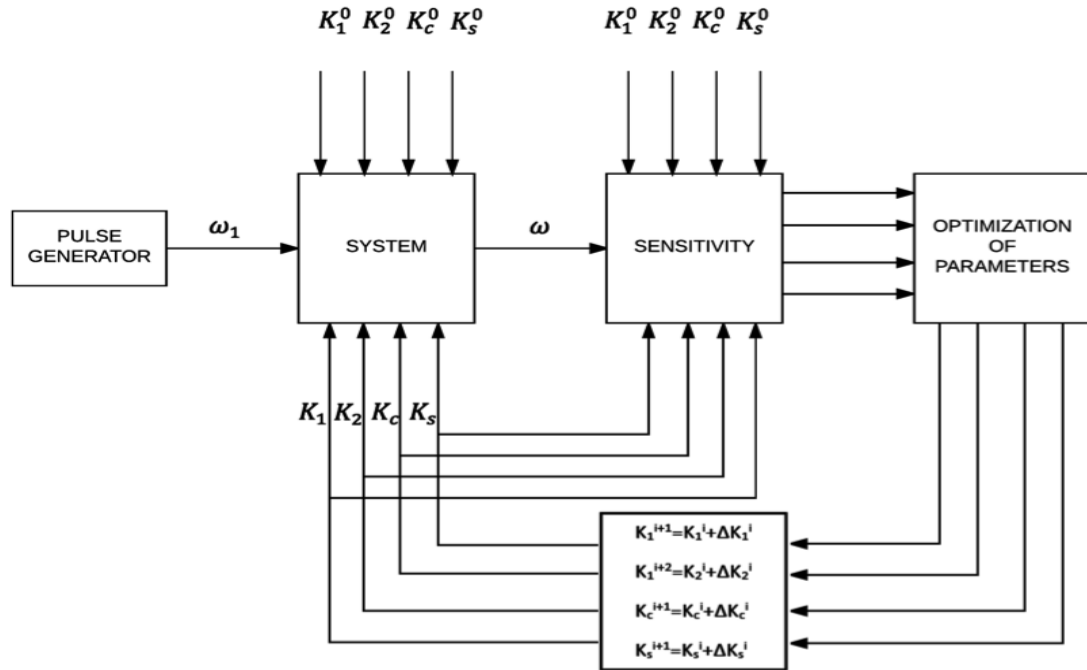


Figure 5.2: Parameter Adjustment.

Each block in Fig 5.2 [13] is developed separately as the parameter adjustment process. The Fig. 5.2 gives a visual picture of the iterative process consisting of calculation of sensitivity coefficients, gradients and parameter or gain update.

## CHAPTER 6: Optimization Strategy with the Proposed Approach

### 6.1 Overview

The procedure for optimization of the response of a system is given in detail in the chapter. The blocks including motor drive system model, sensitivity model and parameter update model are connected and synchronized to give an optimal parameter values. A time delay is applied and the optimal parameter values is given to the motor drive system to analyze the optimized response.

### 6.2 Optimization Strategy

In the following Fig 6.1, the concept of sensitivity analysis based optimization of the system parameters is given and is explained in a step by step process below. The Fig 6.1 shows the interaction between the optimization process employed to obtain the optimal parameter values of a system and the actual system in real-time.

Block A is the optimization strategy used in our study. It consists of the mathematical model of the system, the sensitivity model and the optimization algorithm. Block B consists of the parameter gradient values from Block A, weighting factors for scaling and the parameter value update process.

Block C represents the actual system operating in real-time, waiting to receive the optimal parameter values calculated in A and B.

The offline system [13] minimizes the criterion of the state variables  $\omega$  and  $I_a$ . The criterion is the difference between the reference system desired response and the system actual response. For the system response angular velocity is considered. The criterion is taken as the performance index, which is the square error of the angular velocity and armature current. Based on the performance index, gradient components of the parameters are calculated. As discussed in Chapter 3, sensitivity of the



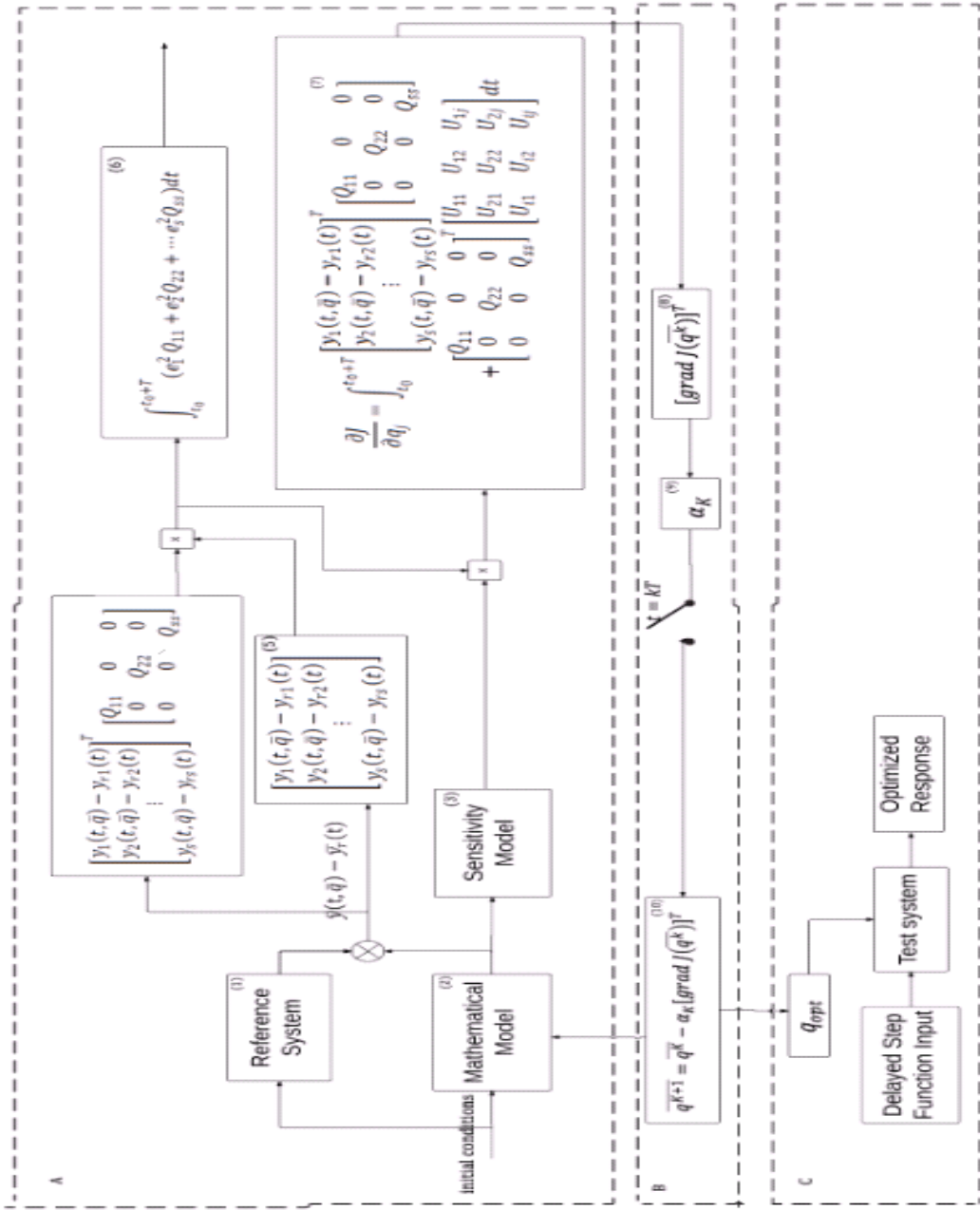


Figure 6.1: Optimization Strategy in Real-Time.

parameters are analyzed to understand the influence on the system. Based on their sensitivity coefficients, sensitivity functions are defined. Using the gradient method, the gradient components of the parameters are calculated and used to minimize the criterion.

A sequence of unit pulses is applied to the system model. When the first step pulse  $u(t)$  is applied to the system model, we monitor the oscillations of the system model response and observe these oscillations dampen to a value smaller than or equal to the tolerance values  $\epsilon_1$  and  $\epsilon_2$  for  $\omega$  and  $I_a$ , respectively. The time period in which this condition is satisfied is defined as  $\Delta t_k$ . For every pulse, a step input is given with the same time interval  $\Delta t_k$ .

For the first pulse given for time interval  $\Delta t_1$ , initial values of the parameters are fed to the system, gradient components of each parameter  $K_1, K_2, K_c, K_s$  are calculated and the parameter values are updated as follows

$$\begin{aligned}
 K_{1new} &= K_{1old} + \Delta K_1 \\
 K_{2new} &= K_{2old} + \Delta K_2 \\
 K_{cnew} &= K_{cold} + \Delta K_c \\
 K_{snew} &= K_{sold} + \Delta K_s
 \end{aligned} \tag{6.1}$$

The updated parameter values from the first interval are updated in the same interval when the pulse goes to zero for a short period before the next pulse is triggered. The updated  $k$  values are applied as input for the next interval.

A second pulse is applied for time interval  $\Delta t_2$ , the mathematical model calculates gradient components with the new  $K_1, K_2, K_c, K_s$  values. An improvement in the response of the system is observed in the second interval. Hence, the parameter values have improved from their initial values. For the second interval the parameter values are updated as given in the aforementioned equations. This process continues

for time intervals  $\Delta t_1, \Delta t_2 \dots$  until the difference in the error of the reference value and a particular iteration reach the tolerance values  $\epsilon_1$  and  $\epsilon_2$  i.e,

$$\omega_r - \omega \leq \epsilon_1$$

$$I_{ar} - I_a \leq \epsilon_2$$

This process produces an optimal response of the angular velocity  $\omega$  of the system under study.

The process of optimization of parameters in real-time is given in Fig 6.1 and is explained in detail here. In each of the iterations, the model of the reference system in block 1 gives the desired output  $\bar{y}_r(t)$ . This output is compared with an output from the mathematical model in block (2)  $y(t, \bar{q})$ , defining the error. In further calculation in blocks (3), (4), (6) and (7), criterion  $J(\bar{q}^k)$  is calculated according to equation 2.1. The transpose of the error  $y(t, \bar{q})$  in block (4) is then multiplied with the product of the error and the weighting matrix Q. The weighting matrix Q is used to normalize the error on common scale.

With sensitivity model (3) and blocks (4) and (7), the criterion is calculated by multiplying the sensitivity function in block (3) and the error. The gradient of the criterion (8)  $gradJ(\bar{q}^k)$  is calculated according to equation 2.4. These calculations are detailed in the blocks A and B. After the simulation is finished at parameter  $\bar{q}^k$ , in the blocks (9), (10) and (12), the new parameters  $\bar{q}^{(k+1)}$  are calculated and the procedure is repeated until  $\bar{q}_{min}^{k+1}$ . It is convenient that all of the integrations in blocks (1), (2), (3), (6) and (7) are done simultaneously, i.e, the part of the diagram, (A) is considered as one system. Part B of the block diagram shows the iterative procedure for parameter calculation. Part C is the system with the finally adjusted parameters and waits with a delay of  $k\Delta t$  ms during the calculation in (A) and (B), i.e, its not active until the calculation in blocks (A) and (B) is complete. If A and B is complete in  $k\Delta t$

ms where  $k$  is the number of iterations, block (C) will be activated in  $(k\Delta t) + 1ms$ . Initially, step function input will be time delayed into block (C) after  $k\Delta t$ .

Starting from the initial parameters, gradient of the performance index are calculated and the parameters are changed by the gradient value of the performance index to get improved parameters. This is the first iteration. The optimal parameter values are obtained over a course of iterations until the criterion condition ( equation 2.1 ) is satisfied. For the  $k + 1$  iteration, the parameter vector is calculated based on the parameter vector in the previous  $k$  iteration.

$$\bar{q}_{k+1} = \bar{q}_k - \alpha_k [\text{grad}J(\bar{q}_k)]^T \quad (6.2)$$

Sequences of step input pulses are applied. Between each of the pulses there is a dead zone of 1 ms. The system is excited with each separate step pulse with the response just for the time interval 49 ms. In other words, the system has a sequence of excitations and between these excitations, there is no interaction between the system responses. The time interval of 49 ms depends on the system time constant and is determined based on the angular velocity value at the end of each time interval i.e.

$$\omega_r - \omega \leq \epsilon_1 \quad (6.3)$$

$$I_{ar} - I_a \leq \epsilon_2$$

where  $\epsilon_1$  is a set tolerance, the time interval  $\Delta t$  is determined as  $t_{k+1} - t_k$  for each step pulse starting with  $t_0$ ,  $k = 0$ , we have system response  $\omega(t_k)$  and the error between reference response and the actual dynamic response. For the next pulse in the sequence, the system response improves dynamically with changes in the parameter values which are adjusted with the gradient components of the performance index at each iteration. The parameter values are adjusted with the gradient components

of performance index. Blocks A and B describe the structure consisting of these parameter adjustments.

The third pulse applied and the following pulses coming in the sequence will produce response with new parameter adjustment. Continuing the parameter adjustment a point will be reached at which the error  $\omega(t) - \omega_r$  between two consecutive iterations will change negligibly. The change in  $q_j$  parameter values between consecutive iterations will be minimal at this point and can be neglected.

When the gradient components of  $\omega$  and  $I_a$  match the tolerance values, the procedure is stopped and the parameters are identified as optimal. After the optimal results of the parameters from block A are evaluated offline, optimal parameter values are sent to the system working in real-time to get an improved dynamic response for both  $\omega$  and  $I_a$ .

### 6.3 Time Delay Induced into the Real-Time System

The step response applied to the real-time system in block C has a time delay. This time delay has the value  $k\Delta t$ . The total time taken for parameter identification is  $k\Delta t$ . This ensures that system working in real-time, block C, will receive optimal value of the parameters since  $k\Delta t$  is the total time taken for the optimization of parameters after which block C starts operating.

$$u(t_{k+1} - t_k) \tag{6.4}$$

where

$$\Delta t = t_{k+1} - t_k, \text{ for all } k \quad k = 0, 1, 2, \dots \tag{6.5}$$

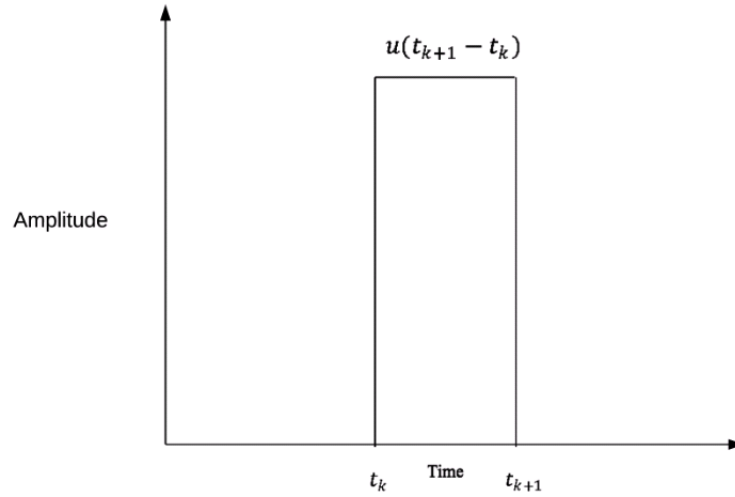


Figure 6.2: Delayed Input

In the next chapter, the proposed approach of  $\omega$  and  $I_a$  based optimization is implemented in a test case. The numerical results of parameter sensitivity analysis, parameter gradient components, parameter value update and integral squared error are shown and explained in detail. The proposed approach is compared to prior work and the improvements are quantified.

## CHAPTER 7: IMPLEMENTATION

### 7.1 Overview

In this chapter implementation of the optimization procedure proposed in this thesis and numerical results are presented. Initial parameter values are taken from reference [13]. Gains are the only parameters to be adjusted, the time constants are not considered since this example is based on Fig 2.2 with the idea that adjustment is made in real-time. However, a similar approach could be used for calculating optimal parameters of the time constants. the only adjustment would consist o the fact that selection of sensitivity variables and the blocks, which deliver the outputs for time constant adjustment will be different. In that case, parameters will be optimized during the design of the drive. The results from the proposed approach is quantified and compared with the prior approach. It is also implemented in different scenarios like mechanical transient and speed variation to analyze improvement in the dynamics of the system.

### 7.2 Implementation in the Test System

The whole procedure is given in Fig 6.1. The system model will be excited with the pulse generator length equal to the system settling time. For the case studies presented, settling time with desired accuracy is less than  $50ms$ . Let's assume it to be 49 ms. After 49 ms, the response reaches steady state with the expected accuracy. The  $k^{th}$  pulse between the time interval  $t_k$  and  $t_{k+1}$  is given in Fig 6.1 in chapter 6 which is displayed again for convenience in Fig 7.1

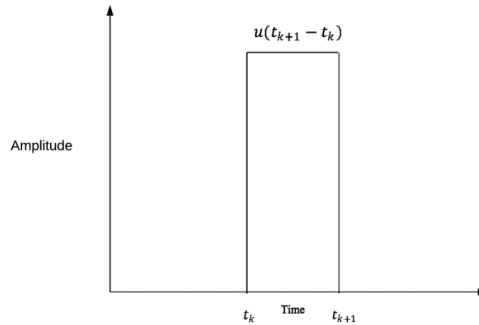


Figure 7.1: Delayed Input

Sequence of pulses will be applied until the parameters in two consecutive iterations are close enough to each other, the difference between the parameter value in two consecutive pulses are less than or equal to tolerance  $\epsilon_2$

### 7.3 Numerical Results of the Proposed Approach

- Sensitivity Function and Gradient Component Changes of the System Gains

In this section, sensitivity coefficients  $V_1, V_2, V_c, V_s$  for gains  $K_1, K_2, K_c, K_s$  respectively are given below. The sensitivity relative to the variation in the output can be observed. Fig 7.2 shows the sensitivity coefficients for the 4 gains for the first 12 pulses. The sensitivity functions for the gains are calculated using equation 3.15 which is repeated here for convenience.

$$T_j(s) = \frac{q_j}{W_j(s, q_i)} \frac{\partial W_j(s, q_j)}{\partial q_j} \quad (7.1)$$

The sensitivity coefficients  $T_1, T_2, T_3$  and  $T_4$  of the parameters  $K_c, K_s, K_1$  and  $K_2$  respectively are

$$T_1 = T_2 = T_3 = T_4 = 1 \quad (7.2)$$



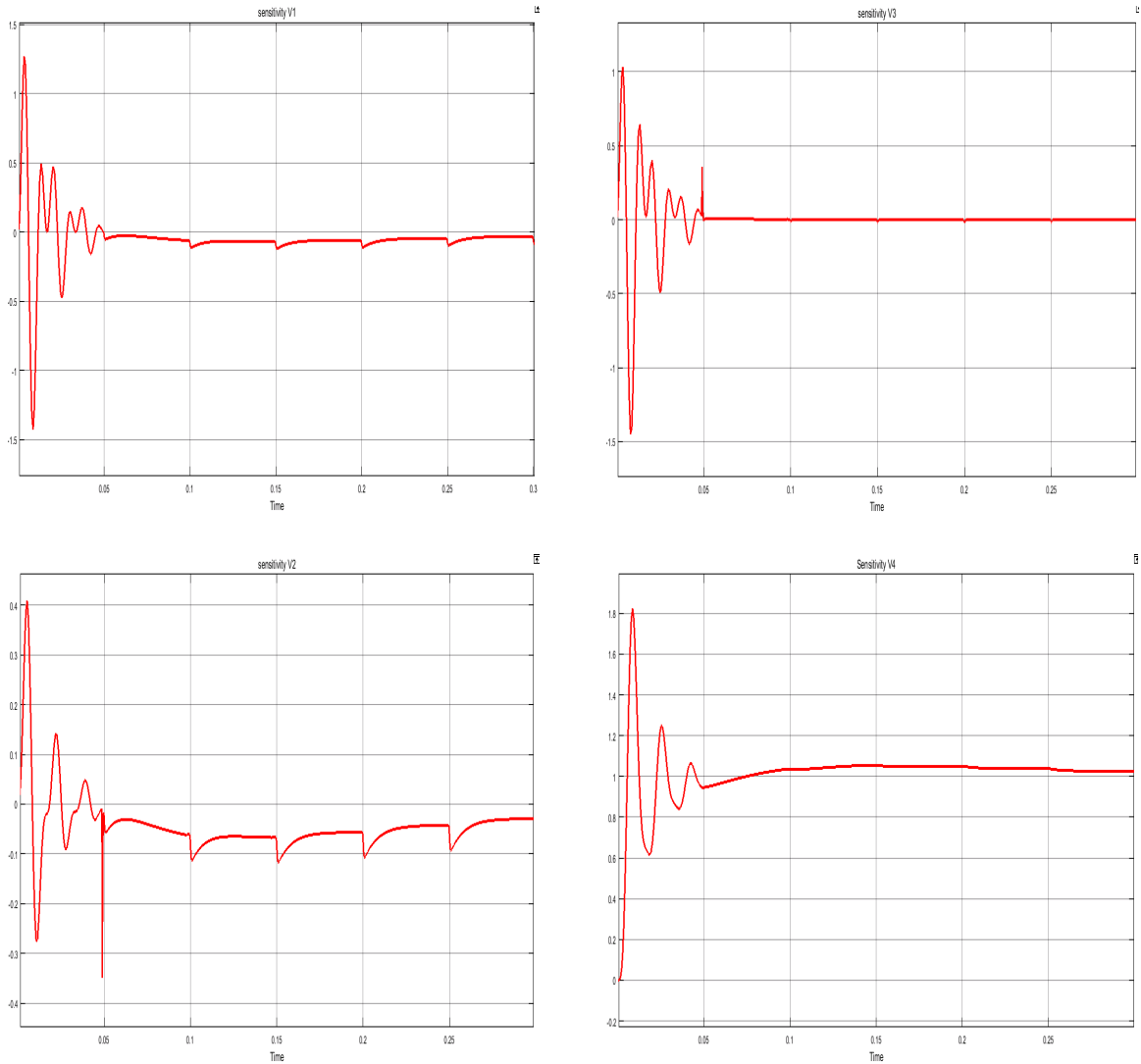


Figure 7.2: Sensitivity coefficients  $V_1$ ,  $V_3$ ,  $V_2$ ,  $V_4$  for gains  $K_1$ ,  $K_2$ ,  $K_c$ ,  $K_s$

- Calculation of the Performance Index Gradient Component

In Fig 7.3, the gradient components are given for our parameters  $\Delta K_1$ ,  $\Delta K_2$ ,  $\Delta K_c$ ,  $\Delta K_s$  over a course of 12 iterations.

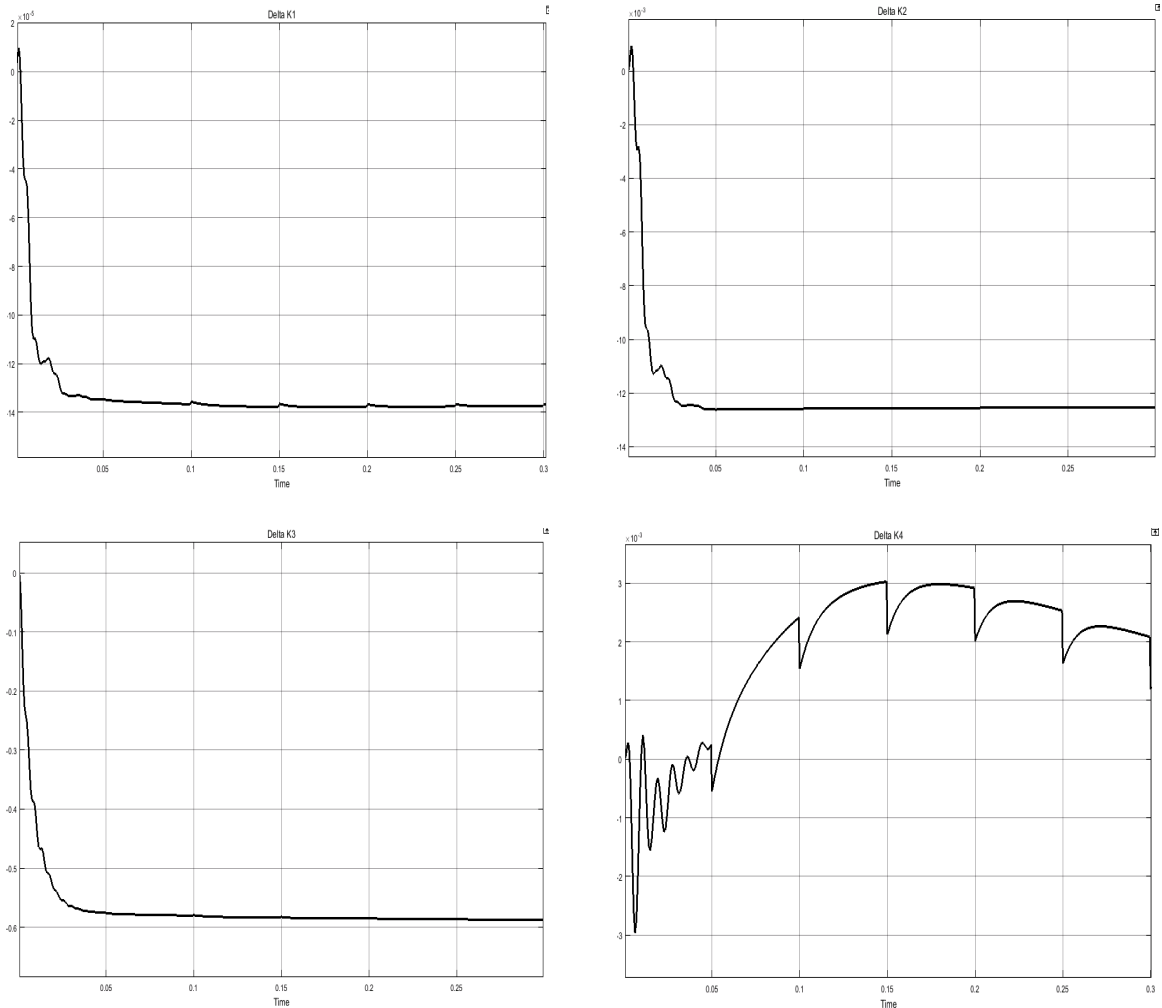


Figure 7.3: Gradient components  $dK_1$ ,  $dK_2$ ,  $dK_c$ ,  $dK_s$  for gains  $K_1$ ,  $K_2$ ,  $K_c$ ,  $K_s$

At the end of each time interval  $\Delta t_k = t_{k+1} - t_k$ , gradient components of the performance index for the 4 gains are calculated. We have sampled the output of the zero-order hold final value of the gradient components. This final value is the change in the gains at the end of each time interval. In our case, after 6 intervals the difference of the parameter changes between 6 and 5 iteration is less than the desired accuracy; therefore, we stop iterating and the optimum values for  $\omega$  and  $I_a$  have been reached. We are interested in only the final value of these changes at the end of the interval.

- Sampled values of the gradient components and parameter update

Fig 7.4 shows the sampled values of the parameters using zero-order hold and the parameter value updated over a course of 6 iterations here.

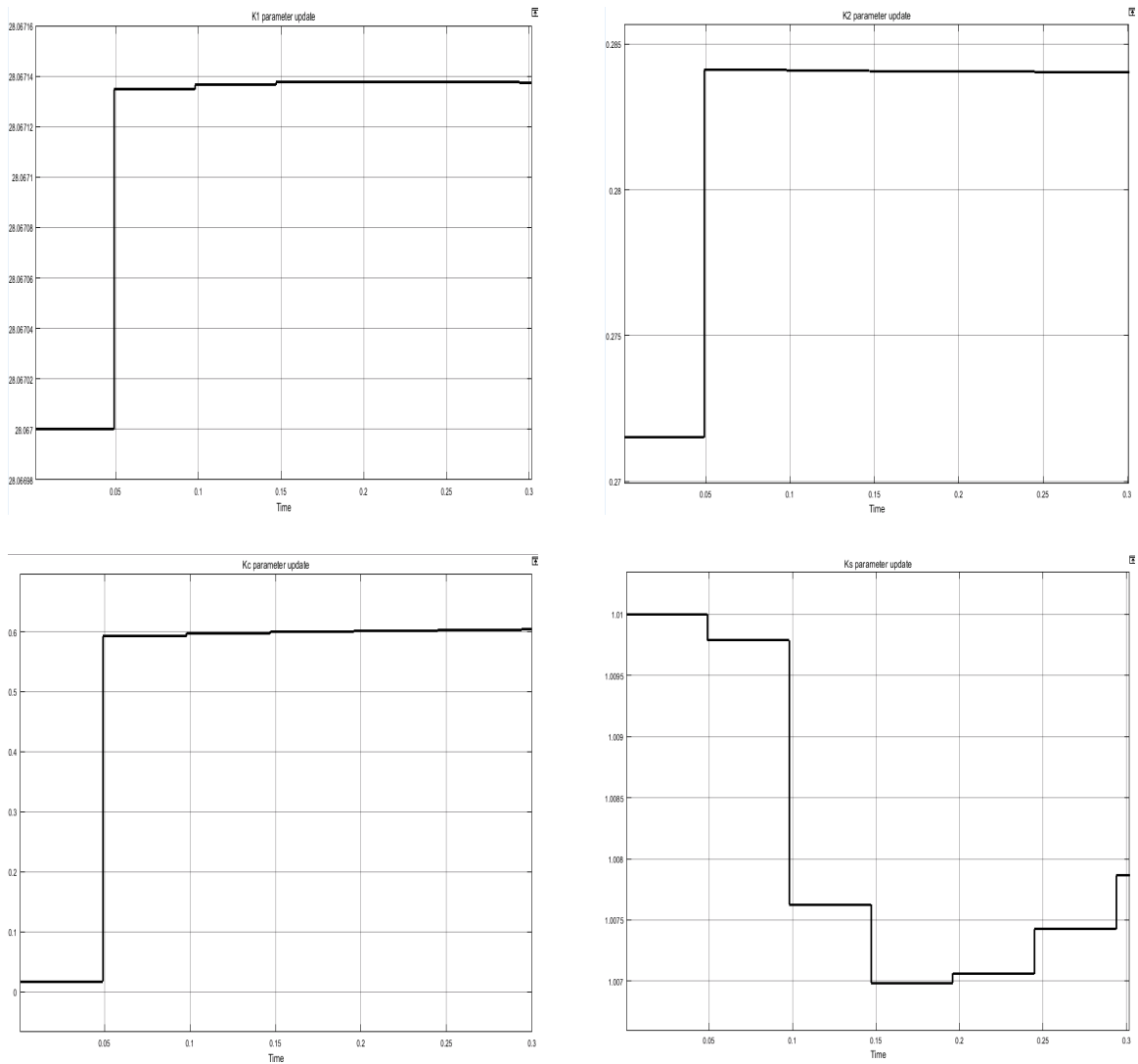


Figure 7.4: Updated parameter signals for gains  $K_1$ ,  $K_2$ ,  $K_c$ ,  $K_s$

The updated values of the gains after each iteration are plotted in Fig 7.4. The values of  $\Delta K_1$ ,  $\Delta K_2$ ,  $\Delta K_c$ ,  $\Delta K_s$  are sampled and held at 49 ms until the next pulse is triggered.

- System Response of Angular Velocity and Armature Current

Improvement in the dynamic response of angular velocity  $\omega$  and armature current  $I_a$  is plotted over 10 time intervals with a time period of 49 ms each in Fig

7.5 and Fig 7.6 respectively

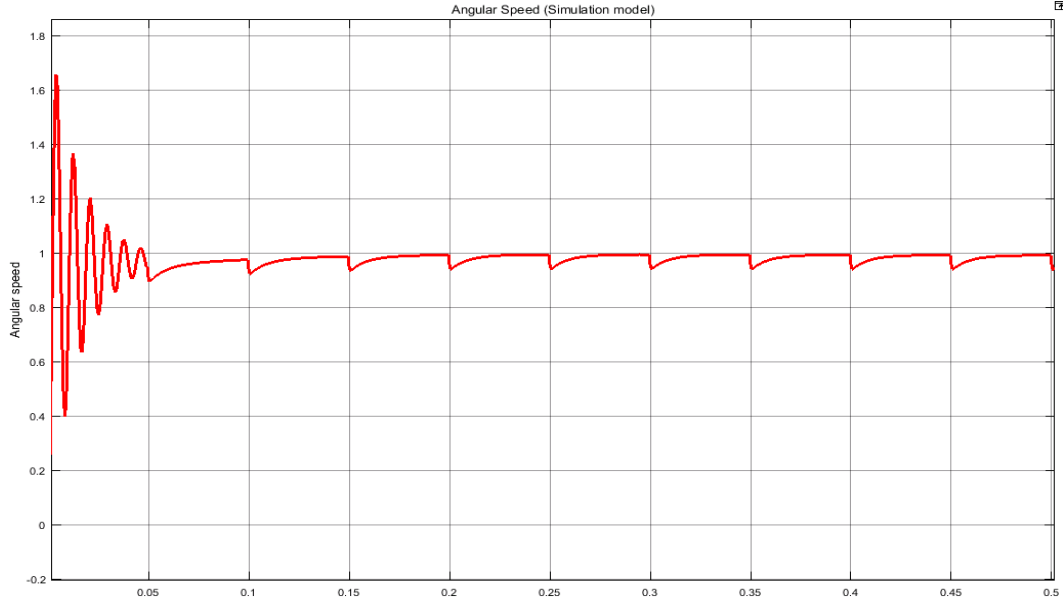


Figure 7.5: Optimization of Angular speed  $\omega$

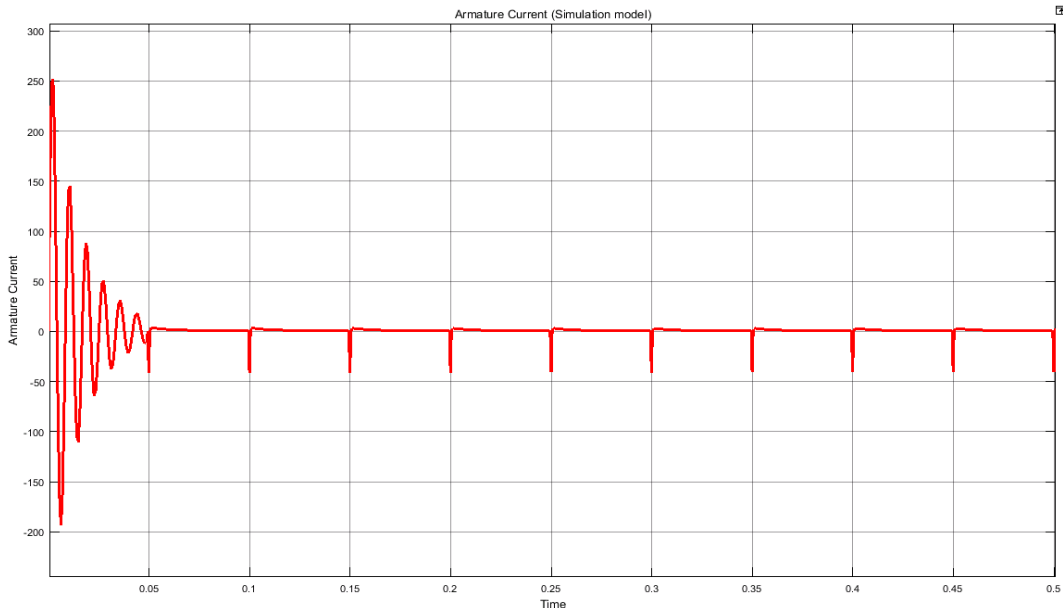
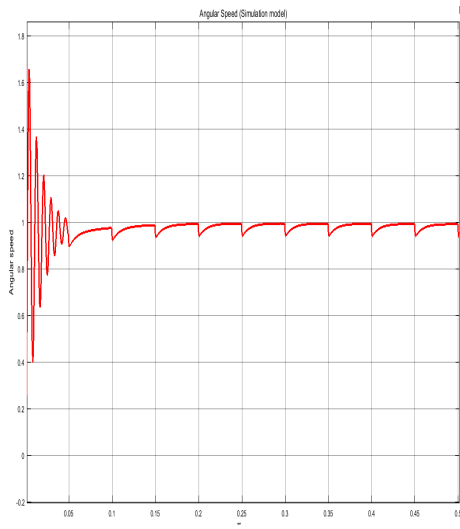


Figure 7.6: Optimization Armature Current  $I_a$

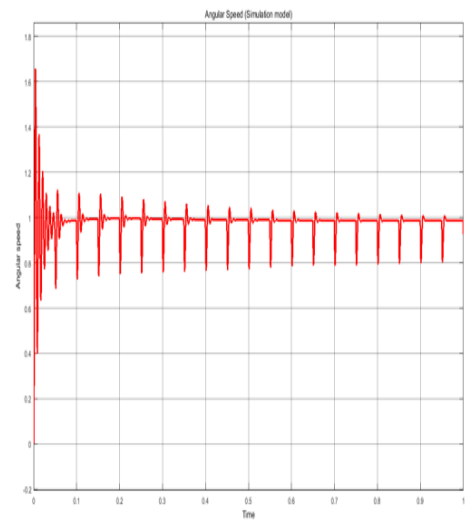
#### 7.4 Comparison of $\omega$ and $I_a$ -Based Proposed Approach with $\omega$ -Based Existing Approach

In Fig 7.7, the results of angular velocity  $\omega$  and armature current  $I_a$  for the proposed approach  $\omega$  and  $I_a$  method and the existing approach  $\omega$  based method are

given respectively in (a) and (c), and (b) and (d).



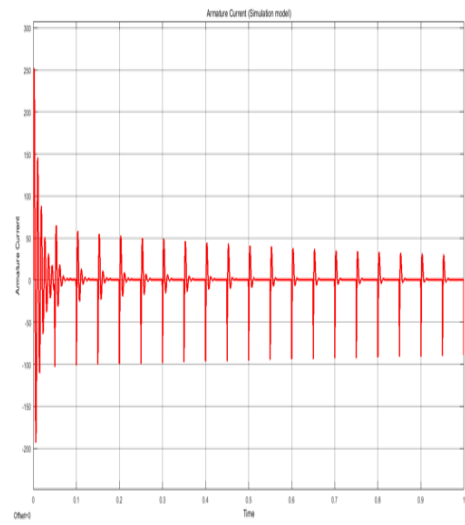
(a) Angular velocity  $\omega$



(b) Angular velocity  $\omega$



(c) Armature current  $I_a$   
Proposed Approach



(d) Armature current  $I_a$   
Existing Approach

Figure 7.7: Comparison of optimization results

With the proposed approach, the optimal values for  $\omega$  and  $I_a$  reach their optimal values in 0.5 s with mitigated oscillations compared to the existing approach where the optimal values are obtained in 1 s with significantly more oscillations.

Hence, the proposed approach has a better and higher convergence rate compared to the existing one, and it also gives a better dynamic response with minimal initial

swings.

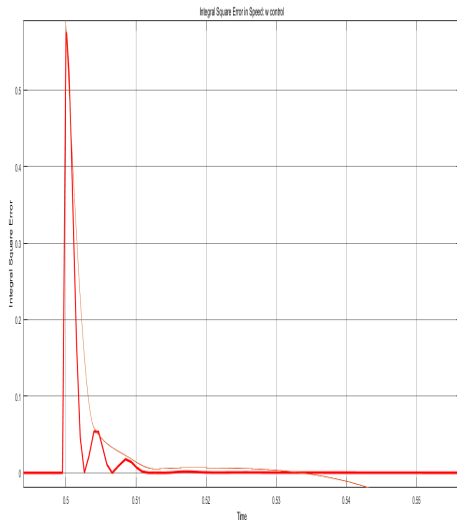
- Comparison of Integral Squared Error of the Approaches

The Integral Squared Error (ISE) for the existing speed based approach and, proposed speed and armature current approach were computed. The Integral Squared Error is the performance index that is used to find the optimal values of the gains  $K_1$ ,  $K_2$ ,  $K_c$  and  $K_s$  and is given by

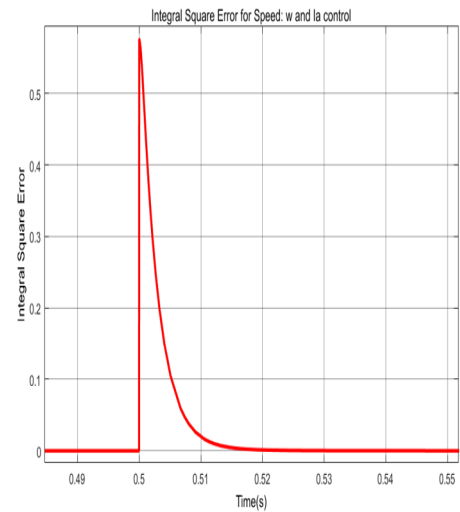
$$J = \int_{t_0}^{t_0+T} e_1^2 \omega + e_2^2 I_a dt$$

- Comparison of Approaches: ISE of  $\omega$  only

The waveform of ISE of angular velocity obtained for both the approaches are analyzed in Fig 7.8.



(a) Angular velocity  $\omega$   
Existing Approach



(b) Angular velocity  $\omega$   
Proposed Approach

Figure 7.8: Comparison of Approaches: ISE of  $\omega$  only

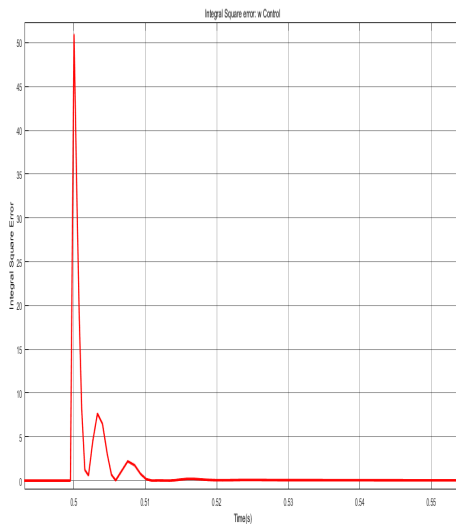
The peak error is reduced by a small value of 0.87 % and the steady state error is considerably minimized by 55 %. The waveforms are quantified in the Table 7.1 below.

Table 7.1: Analysis: ISE of  $\omega$ 

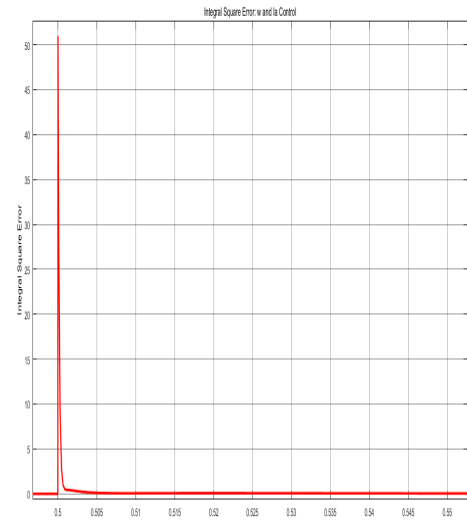
Parameter	$\omega$ based control	$\omega$ and $I_a$ control
Error peak	0.581	0.5759
Time constant (s)	0.002	0.0031
Steady state error	1.9e-4	8.4e-5

- Comparison of Approaches: ISE of  $I_a$  only

The integral squared error of armature current only, for both the approaches is given in Fig 7.9(a) and 7.9(b) respectively.



(a) Armature current  $I_a$   
Existing Approach



(b) Armature current  $I_a$   
Proposed Approach

Figure 7.9: Comparison of Approaches: ISE of  $I_a$  considered separately

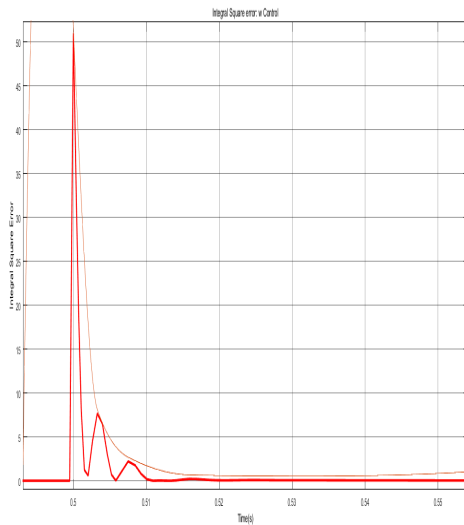
With the proposed approach, the initial swings are considerably minimized and the oscillations are also damped at a higher rate within a short period of time. Table 7.2 below quantifies integral squared errors of both the approaches comparing their peak error, time constant, oscillation damping time and steady state error.

Table 7.2: Analysis: ISE of  $I_a$ 

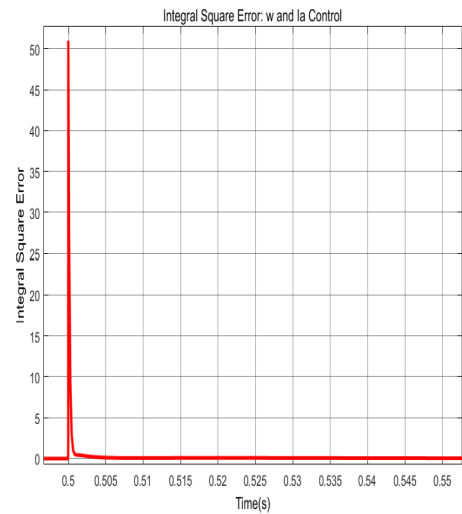
Parameter	$\omega$ based control	$\omega$ and $I_a$ control
Error peak	50.97	50.97
Time constant (s)	0.002	0.0002
Oscillation damping time (s)	0.01	0.001
Steady state error (s)	0.05476	0.07211

- Comparison of Approaches: ISE of the Performance Index

The integral squared error in Fig 7.10 is the performance index used in this thesis. It is the combined integral squared errors of  $\omega$  and  $I_a$ .



(a) Angular velocity  $\omega$   
Existing Approach



(b) Angular velocity  $\omega$   
Proposed Approach

Figure 7.10: Comparison of Approaches: ISE of the Performance Index

The value of this performance index is used to calculate the optimal gain values. Table 7.3 compares the parameters analyzed for both approaches, proving the effectiveness of the proposed approach.



Table 7.3: Analysis: ISE of the Performance Index

Parameter	$\omega$ based control	$\omega$ and $I_a$ control
Error peak	50.97	50.94
Time constant (s)	0.002	0.0002
Oscillation damping time (s)	0.01	0.0001

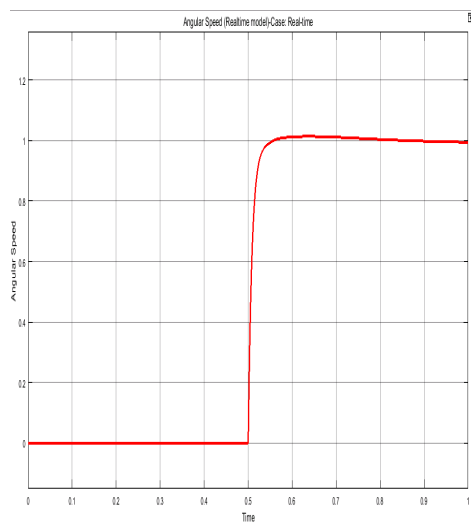
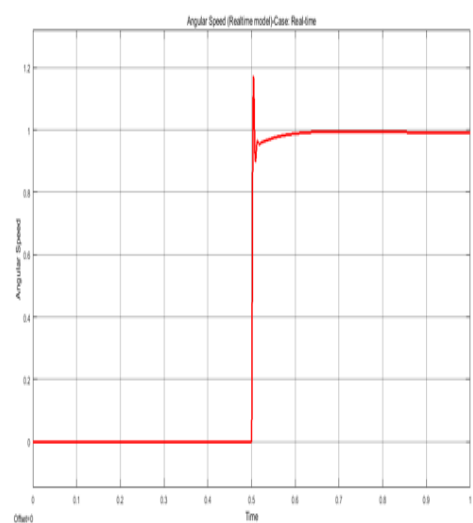
## 7.5 Case Studies

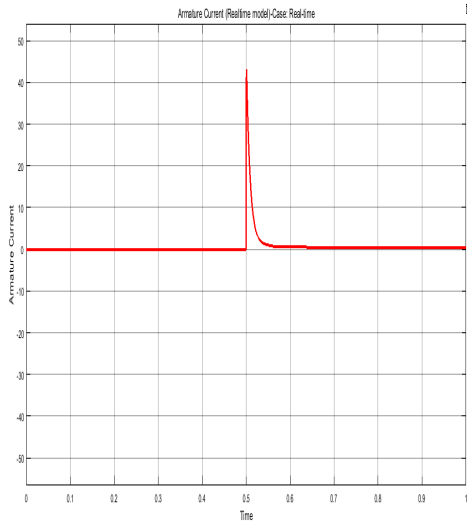
The optimization of system parameters is implemented in 3 example cases:

1. real-time system
2. mechanical transient
3. variable speed control

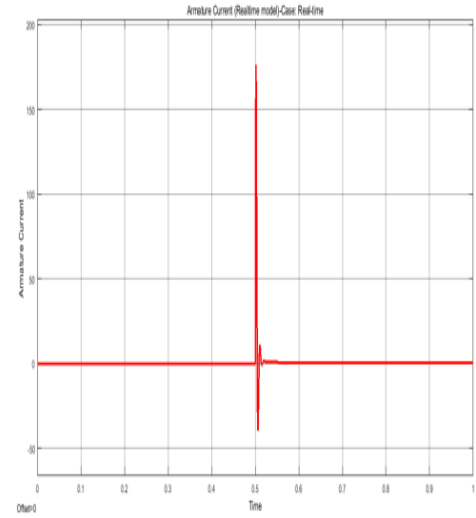
### 7.5.1 Case 1: Real-Time System

When the parameters reach their optimal values after a course of iterations, their optimum values are fed to the real-time system to obtain an optimized response. Hence, initial swings in the real-time system are considerably minimized in Fig 7.11.

(a) Angular velocity  $\omega$ (b) Angular velocity  $\omega$



(c) Armature current  $I_a$   
Proposed Approach



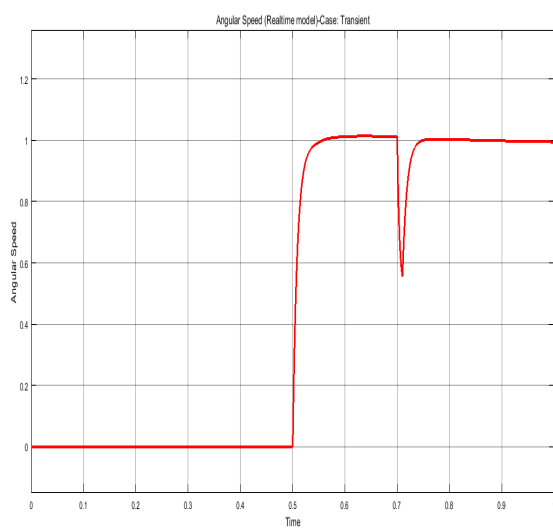
(d) Armature current  $I_a$   
Existing Approach

Figure 7.11: Comparison of Approaches: Real-Time System Output of  $\omega$  and  $I_a$

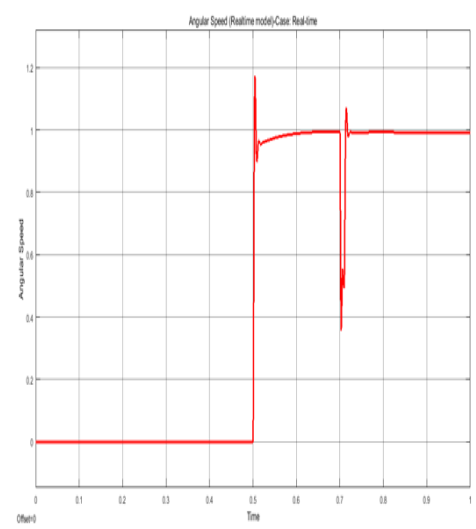
In Fig 7.11, the overshoot in angular velocity is reduced by 15% and the overshoot in armature current is reduced by 76% compared to the existing approach, using the proposed approach.

### 7.5.2 Case 2: Mechanical Transient Response in a Real-Time System

Under a sudden random change in the mechanical loading of the DC motor, may be induced a transient in the normal operation.



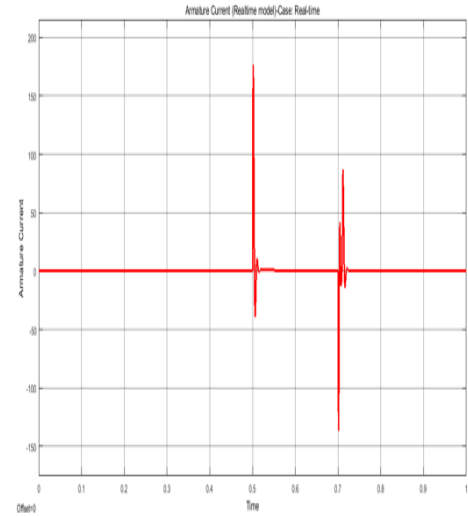
(a) Angular velocity  $\omega$



(b) Angular velocity  $\omega$



(c) Armature current  $I_a$   
Proposed Approach



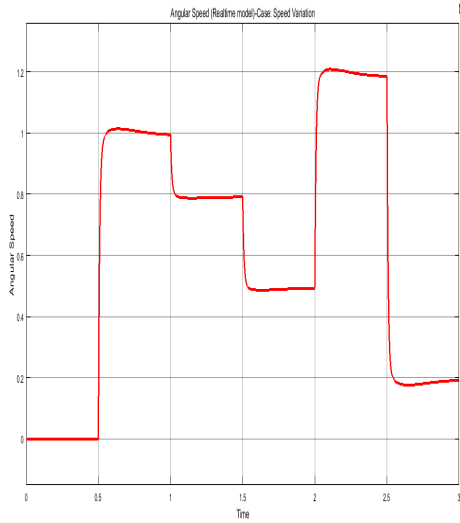
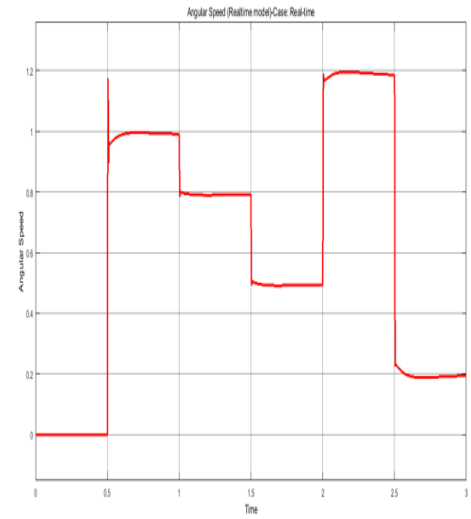
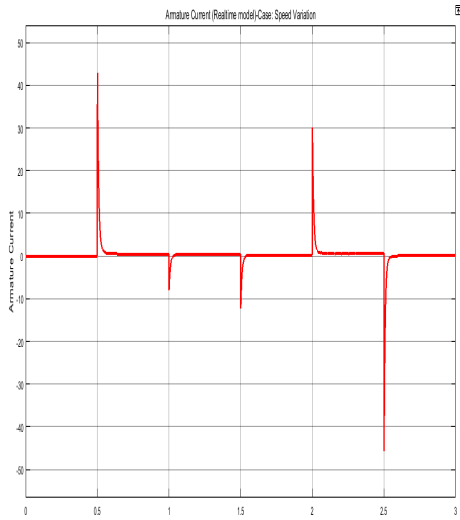
(d) Armature current  $I_a$   
Existing Approach

Figure 7.12: Comparison of Approaches: Transient Response of  $\omega$  and  $I_a$

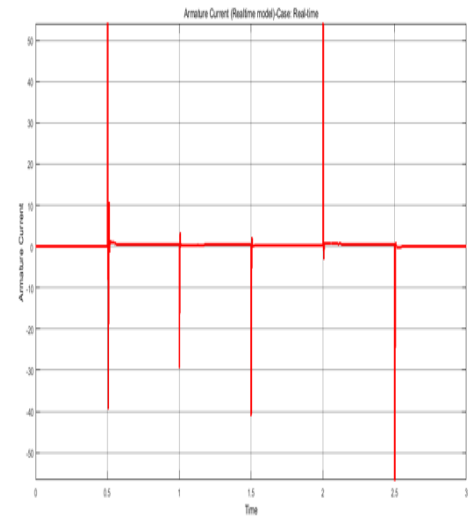
The separately excited DC motor, being a constant speed motor, undergoes oscillations while recovering from transients. Optimized gain values of the regulator parameters result in a quick recovery from the transient conditions with minimal swings. This is shown in Fig 7.12. In Fig 7.12, the overshoot in angular velocity is reduced by 76% and the overshoot in armature current is reduced by 42% using the proposed approach.

### 7.5.3 Case 3: Speed control in a Real-time system

When speed control is employed for speed variation in the DC motor, the changes are accompanied with initial swings because of the momentum. The optimal gain values are adjusted dynamically to provide a smooth angular speed shift. The responses for angular speed and armature current are shown in Fig 7.13.

(a) Angular velocity  $\omega$ (b) Angular velocity  $\omega$ (c) Armature current  $I_a$ 

Proposed Approach

(d) Armature current  $I_a$ 

Existing Approach

Figure 7.13: Comparison of Approaches: Response of  $\omega$  and  $I_a$  to speed variation

The angular speed is varied to 80% between 1 s to 1.5 s, 50% between 1.5 s to 2 s, 120% between 2 s to 2.5 s and 20% between 2.5 s to 3 s, of the reference speed. In 7.15, the separately excited DC motor has a smooth angular shift and the system copes with the changes quickly in Fig 7.16, the spikes are considerably reduced. It can be seen that there is a smooth transition between speed changes in the responses of both  $\omega$  and  $I_a$ . When the speed change is applied via reference signal magnitude,

the new gain values are computed in the simulation model and fed dynamically to the real-time model and hence a spontaneous change in speed is observed.

In the next chapter, conclusion is given in detail with summary of contributions made in this work. An idea of possible future work is also given in brief.

## CHAPTER 8: CONCLUSION

### 8.1 Conclusion and Summary of Contributions

The dynamic response of the DC motor drive system was improved by optimizing parameters with respect to angular velocity  $\omega$  and armature current  $I_a$  when compared to response of the system by optimizing the parameters with respect to  $\omega$  only. The parameter values were improved over a course of iterations via sensitivity based parameter identification. The parameters under consideration were updated to a new improved value by adding performance index gradient components of the parameter in each iteration until the optimized response was achieved. This update was carried out by calculating the sensitivity coefficients of the parameters and using them to determine the gradient components. The performance index (PI) used in this approach is the combined integral squared error of angular velocity  $\omega$  and armature current  $I_a$ . This PI gives a higher convergence rate and improves the dynamic response of the system compared to the existing  $\omega$ -based approach.

When the optimized parameter values were reached after a course of iterations, the optimum values were fed to the actual system running in real-time to obtain an optimized response. Hence, swings to the change in dynamic conditions of the real-time system were considerably minimized.

A DC motor, when excited is observed to undergo initial swings before reaching a steady state condition. Such swings are undesirable when precision in operation is required. The oscillations are considerably minimized using the proposed optimal parameter values obtained with respect to  $\omega$  and  $I_a$ .

Under sudden changes in the mechanical loading of the DC motor, transients may be induced in the normal motor operation. The separately excited DC motor, being a

constant speed motor, undergoes oscillations while recovering from transients. The optimized gain values of the regulator parameter help the motor recover quickly from the transient condition with minimal swings.

When speed control is employed for speed variation in the DC motor, the changes are accompanied with initial swings because of the momentum. The optimal gain values are adjusted dynamically to provide a smooth angular speed shift.

Hence the method promises a fast approach for coping with dynamic changes in an efficient way by significantly mitigating oscillations arising due to disturbances in the DC motor system.

## 8.2 Future Work

The proposed approach is applied to a linearized mathematical model in this work. The linear model is accurate as long as the motor rotates in a particular direction. Non-linear parameters, such as dead zone and Coulomb friction, can be approximated using the linear model. The model in this work is accurate for conventional control scenarios. When the motor needs to be rotated in the opposite direction, it has to cross the zero speed point and the non-linear parameters cannot be linearized.

These hard non-linearities cannot be neglected and will result in an inaccurate mathematical model. Hence, a non-linear mathematical model can be developed including the non-linear parameters and the proposed approach can be applied to the model to achieve optimal values of the unknown parameters using Parameter Identification and hence to obtain an optimal dynamic response for the system.

## REFERENCES

- [1] B. Allaoua, B. Gasbaoui, and B. Mebarki, "Setting up pid dc motor speed control alteration parameters using particle swarm optimization strategy," *Leonardo Electronic Journal of Practices and Technologies*, vol. 14, pp. 19–32, 2009.
- [2] A. Rubaai and R. Kotaru, "Online identification and control of a dc motor using learning adaptation of neural networks," *IEEE transactions on industry applications*, vol. 36, no. 3, pp. 935–942, 2000.
- [3] S. Aydemir, S. Sezen, and H. M. Ertunc, "Fuzzy logic speed control of a dc motor," in *Power Electronics and Motion Control Conference, 2004. IPEMC 2004. The 4th International*, vol. 2. IEEE, 2004, pp. 766–771.
- [4] L. E. B. da Silva, G. L. Torres, E. C. Saturno, A. P. A. da Silva, and X. Dai Do, "Simulation of a neural net controller for motor drives," *Mathematics and computers in simulation*, vol. 38, no. 4-6, pp. 311–322, 1995.
- [5] C. M. Fonseca, P. J. Fleming *et al.*, "Genetic algorithms for multiobjective optimization: Formulation discussion and generalization." in *Icga*, vol. 93, no. July. Citeseer, 1993, pp. 416–423.
- [6] P. Albertos and A. Sala, "Fuzzy logic controllers. advantages and drawbacks," in *VIII International Congress of Automatic Control*, vol. 3, 1998, pp. 833–844.
- [7] I. Völlmecke, "Parameter identification of dc motors," *IMC Berlin*, 2013.
- [8] F. Golnaraghi and B. Kuo, "Automatic control systems," *Complex Variables*, vol. 2, pp. 1–1, 2010.
- [9] H. Kwakernaak and R. Sivan, *Linear optimal control systems*. Wiley-interscience New York, 1972, vol. 1.
- [10] I. Nagrath, *Control systems engineering*. New Age International, 2006.
- [11] R. Krishnan, *Electric motor drives: modeling, analysis, and control*. Prentice Hall, 2001.
- [12] R. Tomović, *Sensitivity analysis of dynamic systems*. McGraw-Hill, 1963.
- [13] J. B. Hall, "Dc motor drive parameters adjustments and optimization in real time control system," Ph.D. dissertation, University of North Carolina at Charlotte, 2004.
- [14] M. Zhuang and D. Atherton, "Tuning pid controllers with integral performance criteria," in *Control 1991. Control'91., International Conference on*. IET, 1991, pp. 481–486.



- [15] V. Lukic and J. Hall, "A new approach to an optimal adaptive real time dc motor drive control," *analysis*, vol. 539, no. 082, p. 363.
- [16] A. M. Sharaf and A. A. El-Gammal, "An integral squared error-ise optimal parameters tuning of modified pid controller for industrial pmc motor based on particle swarm optimization-pso," in *Power Electronics and Motion Control Conference, 2009. IPEMC'09. IEEE 6th International*. IEEE, 2009, pp. 1953–1959.
- [17] S. S. Saab and R. A. Kaed-Bey, "Parameter identification of a dc motor: an experimental approach," in *Electronics, Circuits and Systems, 2001. ICECS 2001. The 8th IEEE International Conference on*, vol. 2. IEEE, 2001, pp. 981–984.
- [18] W. Wu, "Dc motor parameter identification using speed step responses," *Modelling and Simulation in Engineering*, vol. 2012, p. 30, 2012.
- [19] M. George *et al.*, "Speed control of separately excited dc motor," *American journal of applied sciences*, vol. 5, no. 3, pp. 227–233, 2008.
- [20] T. Krishnan and B. Ramaswami, "A fast-response dc motor speed control system," *IEEE Transactions on Industry Applications*, no. 5, pp. 643–651, 1974.
- [21] P. Meshram and R. G. Kanojiya, "Tuning of pid controller using ziegler-nichols method for speed control of dc motor," in *Advances in Engineering, Science and Management (ICAESM), 2012 International Conference on*. IEEE, 2012, pp. 117–122.
- [22] M. Krstic, I. Kanellakopoulos, and P. V. Kokotovic, *Nonlinear and adaptive control design*. Wiley, 1995.
- [23] T. Furuhashi, S. Sangwongwanich, and S. Okuma, "A position-and-velocity sensorless control for brushless dc motors using an adaptive sliding mode observer," *IEEE Transactions on Industrial electronics*, vol. 39, no. 2, pp. 89–95, 1992.

## APPENDIX A: MATLAB CODE AND MATLAB SIMULINK MODEL

## A.1 MATLAB Code

```
K1=28.067;
K2=0.2715;
Kc=0.017;
Ks=1.01;
init=0;
timestep=.001;
tstop=0.3;
t=[0:timestep:tstop];
T1=0.162;
T2=0.075609;
Ta=0.07561;
Kt=97;
J=1.5988;
B=2;
Ra=0.045;
CE=0.411;
Ce=3.92;
Ke=1;
wref=1;
Tref=1.09;
amp=1;
wi=0.1
ws=0.9
sim('Final1');
```

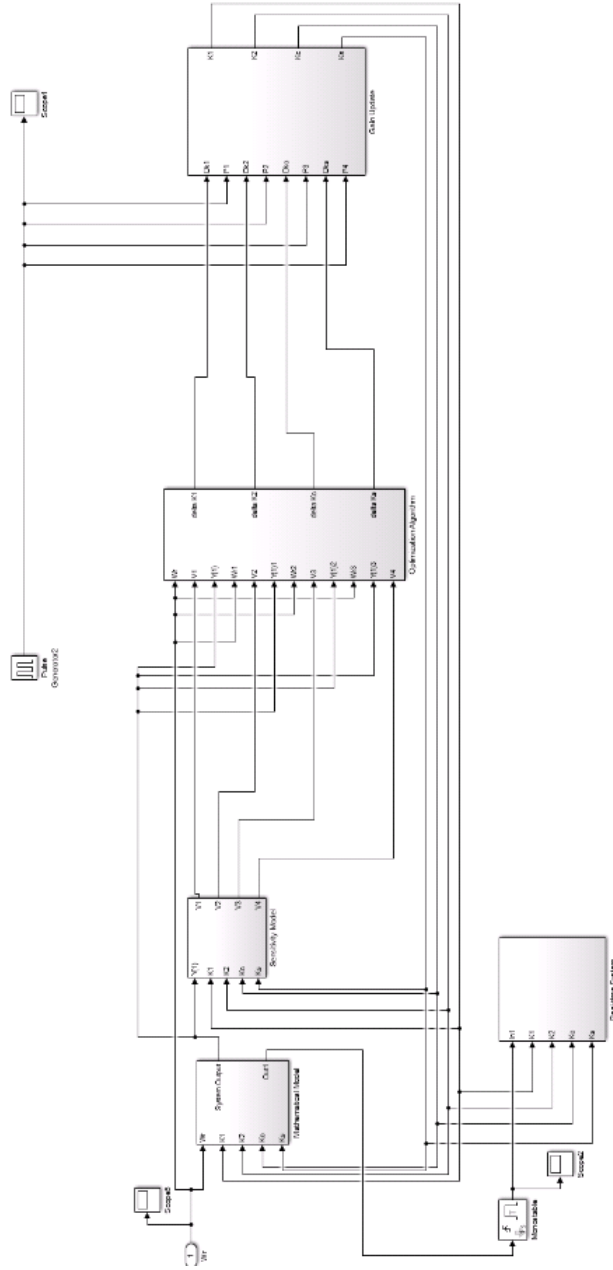


Figure A.1: Optimisation Strategy.

## A.2 Optimization Strategy



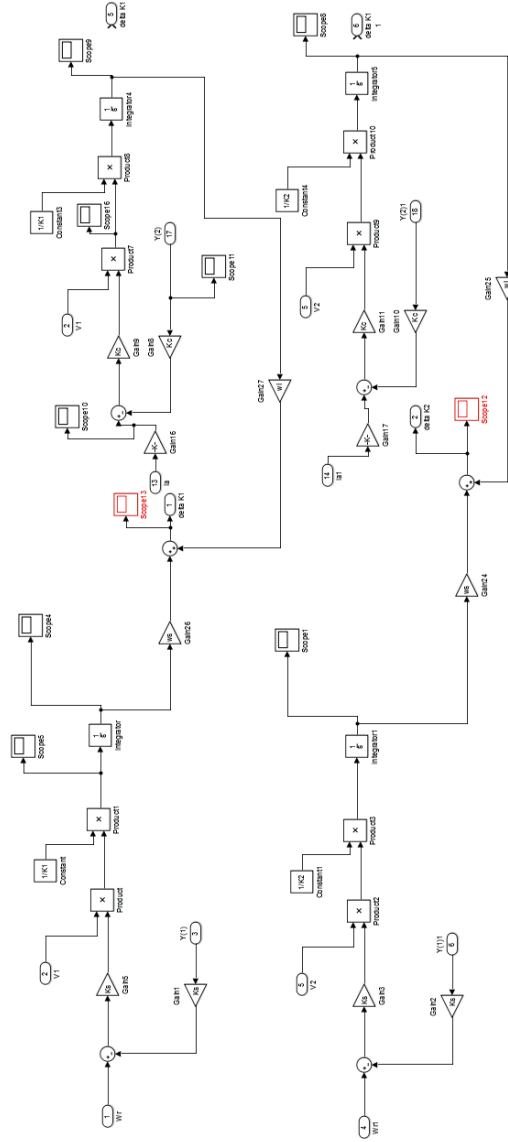


Figure A.3: Gradient Component Calculation.

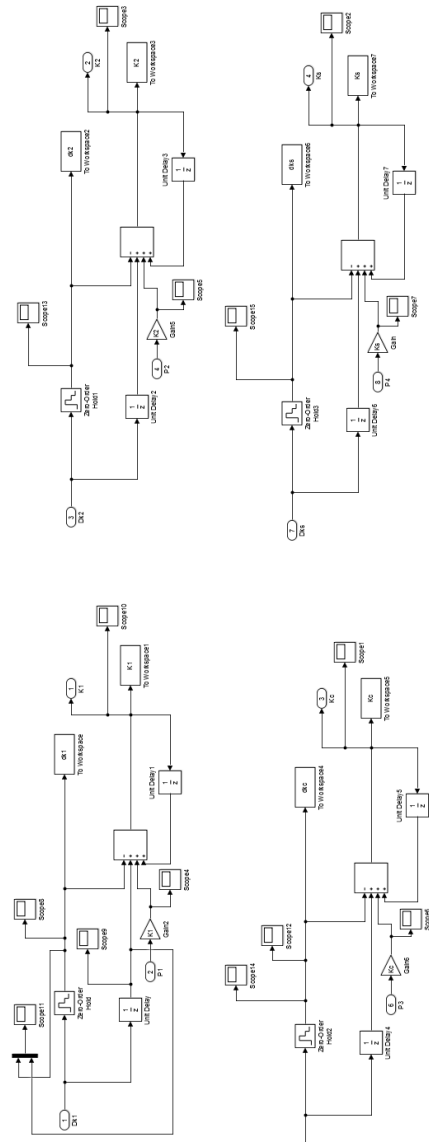


Figure A.4: Parameter Update.

## APPENDIX B: NOTATIONS

$\omega_r$  : reference angular velocity

$\omega$  : Actual angular velocity

$I_{ar}$  : Reference armature current

$I_a$  : Actual armature current

$t_0$  : Initial start time

$T$  : Total time period

$K_1$  : Speed regulator gain

$K_2$  : Current regulator gain

$K_s$  : Angular speed feedback gain

$K_c$  : Armature current feedback gain

$T_1$  : Sensitivity function for  $K_2$

$T_2$  : Sensitivity function for  $K_c$

$T_3$  : Sensitivity function for  $K_1$

$T_4$  : Sensitivity function for  $K_s$

$V_1$  : Sensitivity coefficient for  $K_2$

$V_2$  : Sensitivity coefficient for  $K_c$

$V_3$  : Sensitivity coefficient for  $K_1$

$V_4$  : Sensitivity coefficient for  $K_s$

$r$  : Loops in the sensitivity model

$l$ : Total number of loops in the sensitivity model

$q_{(2r-1)}$ : Parameter for calculation of sensitivity coefficient in feedforward path

$q_{2r}$  : Parameter for calculation of sensitivity coefficient in feedback path

$L(s)$  : Closed loop transfer function

$F(s)$  : Transfer functions

$W_{(2r-1)}(s, q_{(2r-1)})$  : Transfer function of parameter in the feedforward path

$W_{2r}(s, q_{2r})$  : Transfer function containing parameter in the feedback path

$T_{(2r-1)}(s)$  : Sensitivity function of the parameter in the feedforward path

$T_{2r}(s)$  : Sensitivity function of the parameter in the feedback path

$Q$  : Weighing matrix

$J$  : Performance index

$Y(1)$  : Feedback signal for the speed loop

$X(10)$  : Feedback signal for the current loop

$X(14)$  : Input current signal